EUROPEAN ORGANIZATION FOR NUCLEAR RESEARCH (CERN)

CERN-EP-2022-004
2022/08/23

CMS-HIG-20-005

Search for Higgs boson pair production in the four b quark final state in proton-proton collisions at $\sqrt{s} = 13\,\text{TeV}$

The CMS Collaboration*

Abstract

A search for pairs of Higgs bosons produced via gluon and vector boson fusion is presented, focusing on the four b quark final state. The data sample consists of proton-proton collisions at a center-of-mass energy of 13 TeV, collected with the CMS detector at the LHC, and corresponds to an integrated luminosity of $138\,\text{fb}^{-1}$. No deviation from the background-only hypothesis is observed. A 95% confidence level upper limit on the Higgs boson pair production cross section is observed at 3.9 times the standard model prediction for an expected value of 7.8. Constraints are also set on the modifiers of the Higgs field self-coupling, κ_λ, and of the coupling of two Higgs bosons to two vector bosons, κ_{2V}. The observed (expected) allowed intervals at the 95% confidence level are $-2.3 < \kappa_\lambda < 9.4$ ($-5.0 < \kappa_\lambda < 12.0$) and $-0.1 < \kappa_{2V} < 2.2$ ($-0.4 < \kappa_{2V} < 2.5$). These are the most stringent observed constraints to date on the HH production cross section and on the κ_{2V} coupling.

Published in Physical Review Letters as doi:10.1103/PhysRevLett.129.081802.

*See Appendix B for the list of collaboration members

The discovery of the Higgs boson (H) by the ATLAS and CMS Collaborations [1–3] proves the existence of a fundamental scalar sector of the standard model of particle physics (SM), but the experimental confirmation of the Brout–Englert–Higgs mechanism [4–6] requires the determination of the shape of the postulated scalar potential. This shape is governed by a parameter, λ, that drives the strength of the Higgs boson self-couplings and can thus be determined experimentally with a measurement of Higgs boson pair (HH) production.

At the CERN Large Hadron Collider (LHC), at the energy of $\sqrt{s} = 13\,\text{TeV}$, the dominant HH production mode in the SM is through the gluon fusion mechanism (ggF), with a cross section of $31.1^{+2.1}_{-7.2}\,\text{fb}$ [7–14], followed by the vector boson fusion process (VBF), with a cross section of $1.726 \pm 0.036\,\text{fb}$ [15] and characterized by the presence of two additional hadronic jets, j, giving a $\mathrm{b\bar{b}b\bar{b}jj}$ final state. Variations of the Higgs boson self-coupling with respect to the SM prediction are parameterized by the modifier $\kappa_\lambda = \lambda/\lambda^{\text{SM}}$ and affect the ggF and VBF production modes. The VBF production mode also depends on the strength of the interaction of pairs of vector bosons V (= W, Z) with a single (VVH) and a pair (VVHH) of Higgs bosons, whose values with respect to the SM prediction are parameterized by the modifiers κ_{V} and $\kappa_{2\text{V}}$, respectively. Departures from the relation $\kappa_{2\text{V}} = \kappa_{\text{V}}^2$ predicted in the Brout–Englert–Higgs mechanism are possible in models of physics beyond the SM where the Higgs boson is a composite state emerging from the presence of new strong dynamics at the TeV scale [16].

The ATLAS and CMS Collaborations have searched for ggF HH production with a data set corresponding to an integrated luminosity of about $36\,\text{fb}^{-1}$ in a variety of final states [17–26], whose combinations [27, 28] set an observed (expected) upper limit at the 95% confidence level (CL) on the SM production cross section of 7 (10) and 22 (13) times theoretical prediction, respectively. Updated searches have been performed with an integrated luminosity of about $140\,\text{fb}^{-1}$ [29–31], and the most stringent observed limits are from the ATLAS search in the $\mathrm{b\bar{b}}\gamma\gamma$ final state and correspond to 4.2 times the SM prediction, with a value of κ_λ between -1.5 and 6.7 at the 95% CL. The VBF HH production process has been studied in the $\mathrm{b\bar{b}b\bar{b}}$ [32] and $\mathrm{b\bar{b}}\gamma\gamma$ [30] final states by the ATLAS and CMS Collaborations, respectively, and the most stringent observed constraints at the 95% CL correspond to $-0.43 < \kappa_{2\text{V}} < 2.56$ from $\mathrm{b\bar{b}b\bar{b}}$ and 225 times the SM cross section prediction from $\mathrm{b\bar{b}}\gamma\gamma$.

This Letter reports on searches for both the ggF and VBF HH production mechanisms in the $\mathrm{b\bar{b}b\bar{b}}$ decay channel. In the SM, this decay mode is characterized by a combined branching fraction of 0.339 ± 0.008 for $m_{\text{H}} = 125\,\text{GeV}$ [33]. The analysis uses a sample of proton-proton collision (pp) events at $\sqrt{s} = 13\,\text{TeV}$ recorded between 2016 and 2018 with the CMS detector, corresponding to an integrated luminosity of $138\,\text{fb}^{-1}$.

The CMS apparatus [34] is a multipurpose, nearly hermetic detector, designed to trigger on [35, 36] and identify electrons, muons, photons, and hadrons [37–41]. A global event reconstruction "particle-flow" (PF) algorithm [42] combines the information provided by the all-silicon inner tracker and by the crystal electromagnetic and brass-scintillator hadron calorimeters, operating inside a 3.8 T superconducting solenoid, with data from gas-ionization muon detectors embedded in the solenoid iron return yoke, to build τ leptons, jets, missing transverse momentum, and other physics objects [43–45].

Hadronic jets are clustered from the PF objects using the anti-k_{T} algorithm [46, 47] with a distance parameter of 0.4. Jet energy corrections are derived from simulation studies and corrected with in situ measurements to match the energy scale in data and in simulation [44]. Jets originating from b quarks are identified using as a discriminant the output of a deep neural network algorithm (DEEPJET) [48, 49], trained using as input information the properties of the PF constituents of the jets and of the secondary vertices associated with them. For the jets in this search, two working points (WPs) of the DEEPJET discriminant are considered: the medium WP, which yields a b jet identification efficiency of 75% with a corresponding misidentification rate of light flavor and gluon (charm) jets of about 1 (10)%, and the tight WP, which corresponds to a b jet identification efficiency of 58% and to a misidentification rate of about 0.1 (2)%.

Signal processes from ggF HH production are simulated at next-to-leading order (NLO) accuracy in quantum chromodynamics (QCD) with POWHEG 2.0 [50–52], and samples for VBF HH production are generated at leading order (LO) accuracy in QCD using MADGRAPH5_aMC@NLO 2.6.5 [53] for various combinations of couplings. The distributions are scaled by functions of the couplings defined according to the known dependence of the theoretical cross section [54] and added together to model arbitrary coupling combinations, and the total predictions are normalized to the corresponding next-to-NLO (NNLO) cross section [13] for ggF and by the ratio of the next-to-NNLO [15] to LO SM cross sections for VBF. Although not used to model the background, simulated samples for the QCD multijet, $t\bar{t}$, and ZZ backgrounds are used for the optimization of the analysis. For all simulations, the generators are interfaced with PYTHIA 8.226 (2016) and 8.230 (2017–2018) [55], and the CMS detector response is modeled with GEANT4 [56]. The simulated events are weighted to match the distribution of additional pp interactions (pileup) within the same or nearby bunch crossings, relative to the collision of interest, to the one observed in data. See Appendix A for further details on the simulated samples.

The trigger selection for events collected in 2016 requires the presence of four jets with transverse momentum $p_T > 45\,\text{GeV}$ or of two jets with $p_T > 30\,\text{GeV}$ and two jets with $p_T > 90\,\text{GeV}$. For 2017 (2018) data, the presence of four jets above the p_T thresholds of 40, 45, 60, and 75 GeV is required together with $H_T > 300\,(330)\,\text{GeV}$, respectively, where H_T denotes the scalar sum of the transverse momentum of the jets reconstructed in the event. As a consequence of the change in jet trigger thresholds, data collected in 2017 and 2018 are analyzed separately from those collected in 2016.

Offline, events are required to contain at least four jets with pseudorapidity $|\eta| < 2.4\,(2.5)$ and $p_T > 30\,(40)\,\text{GeV}$ for the 2016 (2017–2018) data, respectively. Jets are required to satisfy the tight WP of the PF jet identification algorithm [57, 58], corresponding to an efficiency larger than 99%. If their p_T is below 50 GeV, the medium WP of the pileup discriminant [57] is also required, for a signal jet efficiency of about 90%. If more than four jets satisfy these criteria, the four objects with the largest DEEPJET output are selected. The p_T of these four jets are corrected with a multivariate regression method developed for b jets that improves the determination of the momentum by up to 15% and simultaneously estimates the per jet resolution achieved [59]. After the application of this method, the resolution on the dijet invariant mass for $H \to b\bar{b}$ events reconstructed in this analysis ranges between 11 and 14%. At least three of the selected jets are required to satisfy the medium WP of the DEEPJET discriminant.

Events are rejected if they contain an electron or a muon with $p_T > 15$ and 10 GeV, respectively, and $|\eta| < 2.4$, where these objects must satisfy identification discriminants and criteria that include isolation and impact parameter with respect to the primary interaction vertex. This selection suppresses background events containing leptonic top quark decays.

The two Higgs boson candidates are formed by pairing the four jets. There are three possible pairings of jets, and in each the two Higgs boson candidates, denoted as H_1 and H_2, are defined by the relation $p_T(H_1) > p_T(H_2)$. The (H_1, H_2) pairings are ordered according to the increasing value of a distance parameter $d = |m_{H_1} - k m_{H_2}|/\sqrt{1+k^2}$. The constant k is the ratio of the expected peak positions of the reconstructed Higgs boson masses for events that are correctly paired, $k = c_1/c_2 = (125\,\text{GeV})/(120\,\text{GeV}) = 1.04$. Its value differs from 1 because of the residual jet momentum dependence of the multivariate energy regression that more strongly impacts the softer H candidate. If the difference in the distance parameter of the first and second pairing, Δd, is larger than 30 GeV, corresponding to about two times the resolution on the Higgs boson mass, the pairing with the smallest d is chosen. Conversely, if $\Delta d \leq 30\,\text{GeV}$, the experimental resolution limits the capability to identify the correct pairing based on the invariant masses, and a choice is made between the first and second pairing as the one that maximizes the p_{T} of the two Higgs boson candidates in the four-jet center-of-mass reference frame. This procedure results in a correct jet pairing of about 96% of the selected events in a ggF SM HH sample, and amounts to 82–96 (91–98)% for the different couplings studied in ggF (VBF) signal events.

The two non-b jets in the VBF production events are selected with $p_{\mathrm{T}} > 25\,\text{GeV}$ and $|\eta| < 4.7$, and they must satisfy the tight WP of the jet identification algorithm and the medium WP of the pileup discriminant if $p_{\mathrm{T}} < 50\,\text{GeV}$. For the 2017 data, affected by large noise in the endcaps of the electromagnetic calorimeter (ECAL), jets in the region $2.6 < |\eta| < 3.1$ are additionally required to satisfy the tight WP of the pileup discriminant to mitigate the noise effects. The two VBF jet candidates j_1 and j_2 are chosen as the highest p_{T} jet and the second-highest p_{T} jet that has an opposite η sign with respect to the former.

Events that do not contain such a VBF jet pair are assigned to the ggF category. About 26–28% of ggF events contain additional jets that satisfy the above requirements on the VBF jet candidates, and in order to correctly classify them, a boosted decision tree (BDT) discriminant is trained to separate ggF and VBF HH signal events. The discriminant uses $p_{\mathrm{T}}(\mathrm{H}_1)$, $p_{\mathrm{T}}(\mathrm{H}_2)$, $p_{\mathrm{T}}(\mathrm{j}_1)$, $p_{\mathrm{T}}(\mathrm{j}_2)$, the invariant mass and absolute value of pseudorapidity of the jj system, the angular separation $\Delta R = \sqrt{(\Delta\eta)^2 + (\Delta\phi)^2}$, where ϕ is the azimuthal angle, between the two H candidates and between each H and VBF jet, the absolute value of the polar angles with respect to the beam direction of the two VBF jets in the center-of-mass frame of the six selected jets and the product of the two Higgs boson centralities $\exp\left[-([\eta(\mathrm{H}_1) - \eta_{\mathrm{avg}}]/\Delta\eta)^2 - ([\eta(\mathrm{H}_2) - \eta_{\mathrm{avg}}]/\Delta\eta)^2\right]$, where $\Delta\eta = \eta(\mathrm{j}_1) - \eta(\mathrm{j}_2)$ and $\eta_{\mathrm{avg}} = [\eta(\mathrm{j}_1) + \eta(\mathrm{j}_2)]/2$. The discriminant is trained to separate the SM ggF HH signal from the $\kappa_{2\mathrm{V}} = 2$ VBF signal, in order to optimize both the sensitivity to the anomalous $\kappa_{2\mathrm{V}}$ coupling hypotheses and the correct classification of SM ggF signal events. The value $\kappa_{2\mathrm{V}} = 2$ is chosen because it is representative of the event kinematics in the presence of anomalous couplings, characterized by the large invariant mass of the jj and HH systems. These signals are associated with a large increase of the total cross section that would make them detectable with the available data set. A threshold on the BDT output is chosen to assign events to either the ggF or VBF category. It results in the correct assignment of about 97% of all ggF HH signal events to the ggF category and of about 60 (80)% of SM ($\kappa_{2\mathrm{V}} = 2$) VBF HH events that contain the additional jets to the VBF category.

Events classified as ggF or VBF signal are further divided into subcategories to optimize the sensitivity of the search for anomalous coupling hypotheses. Events in the ggF category are divided into a low- and high-mass category if the reconstructed invariant mass of the HH system, m_{HH}, is below or above 450 GeV, where the boundary is defined according to the kinematic properties of the signal. The latter category efficiently collects SM ggF HH events, while the former increases the acceptance to signals with anomalous κ_λ values. Events in the VBF category are instead divided into a "SM-like" and an "anomalous $\kappa_{2\mathrm{V}}$-like" category depending on the value of the discriminant trained to separate ggF and VBF. The categorization thresholds were chosen to maximize the expected sensitivity to VBF HH signals, and result in the assignment of about 25–30% of the VBF $\kappa_{2\mathrm{V}} = 2$ events to the anomalous $\kappa_{2\mathrm{V}}$-like category and

95% of SM VBF events to the SM-like category.

The large multijet background that originates from QCD and $t\bar{t}$ hadronic processes is estimated from the data using background-dominated regions. Analysis signal (A_{SR}) and control (A_{CR}) regions are defined by requiring $\chi < 25\,\text{GeV}$ and $25 \leq \chi < 50\,\text{GeV}$, respectively, where χ is the distance from the expected peak position of the two Higgs boson candidates' invariant masses and is defined as $\chi = \sqrt{(m_{H_1} - c_1)^2 + (m_{H_2} - c_2)^2}$, where c_1 and c_2 are as defined for the pairing of the four jets. Both A_{SR} and A_{CR} are divided into a four b jet (4b) and three b jet (3b) region by requiring the b jet candidate with the lowest DEEPJET output to satisfy or fail the medium WP of the discriminant, respectively. There are between 5.5 and 11 times more events in the 3b region than in the 4b region, depending on the topological category and data-taking year considered. The overall efficiency for both ggF and VBF signal events to be selected in the A_{SR}^{4b} region ranges from 0.3 to 3% depending on the couplings considered and is minimal for the SM VBF production and for the ggF production with $\kappa_\lambda \approx 5$ due to the interference effects in the HH production that result in low momenta of the Higgs bosons. The signal acceptance is mostly limited by the trigger acceptance and the jet b tagging efficiency.

Background events in the A_{SR}^{4b} region are modeled from events in the A_{SR}^{3b} region. The former represents the sensitive region of the analysis, while the latter provides a sample enriched in multijet background events with similar kinematic properties. Events in A_{SR}^{4b} were analyzed only after all the methods were defined and validated. The normalization is determined by scaling the observed number of events in A_{SR}^{3b} by a transfer factor computed as the ratio of the number of events in the A_{CR}^{4b} and A_{CR}^{3b} regions. Variations of the transfer factor depending on the position in the (m_{H_1}, m_{H_2}) plane are accounted for by measuring it as a function of $m_{\|}$, defined as the projection of the point in the plane on the line $m_{H_1} = (c_1/c_2)\, m_{H_2}$ that is used for the H candidate reconstruction. Higher values of $m_{\|}$ are correlated with a higher average p_T of the selected jets.

Differences in the distributions of several variables between the 3b and the 4b regions are addressed with the BDT-based reweighting method described in Ref. [60], which uses a dedicated metric to identify the phase space regions with the largest differences in the distributions and compute an event weight to correct for them. This method accurately models multiple variables and their correlations, while minimizing issues related to the statistical uncertainties arising from the limited number of events in the two regions. The BDT is trained in the A_{CR}^{4b} and A_{CR}^{3b} regions, and applied to events in A_{SR}^{3b} to model A_{SR}^{4b}.

Trainings of this BDT are performed separately for each ggF and VBF category. All trainings use as inputs the following ten variables: p_T of the four b jets, m_{HH}, the invariant masses and p_T of the H_1 and H_2 candidates, and the absolute value of their pseudorapidity difference ($|\Delta\eta(H_1, H_2)|$). In the ggF category, ten additional variables are used: the magnitude of the scalar ($\sum p_T$) and vector ($p_T(HH)$) sums of the p_T of the four b jets, the angular ΔR separations between the two jets that constitute H_1 and H_2 ($\Delta R^{H_1}(bb)$, $\Delta R^{H_2}(bb)$), the minimal ΔR (ΔR^{min}) and the maximal $|\Delta\eta|$ ($|\Delta\eta|^{max}$) between all the possible b jet pairs, the absolute value of the angle with respect to the beamline of one Higgs boson in the four-jet reference frame ($|\cos\theta^*|$) and of one jet of H_1 in the H_1 candidate reference frame ($|\cos\theta_b^{H_1}|$), the sum of the resolution estimators of the three b-tagged jets with the best DEEPJET value ($\sum R_e$), and the number of these three jets that satisfy the tight DEEPJET WP (N_b^T). In the VBF category, four additional variables are used: the absolute value of the ϕ separation between the two Higgs bosons, the VBF jets invariant mass and absolute value of the η separation, and the output of the production mode BDT discriminant. These variables are chosen as those that best represent the kinematic properties of the events in the 3b and the 4b regions and that provide separation between signal and background and are used in subsequent steps of the analysis.

The training parameters are optimized with a two-step procedure. First, a Kolmogorov–Smirnov distance test is used to ensure that the distributions of the BDT input variables in the target A_{CR}^{4b} region are compatible with the ones in the reweighted A_{CR}^{3b} region. Once that is verified, a BDT is trained to separate the A_{CR}^{4b} and reweighted A_{CR}^{3b} data, thus testing also the correlations of variables. All the training configurations that are chosen are required to have an area of 0.5 under the receiver operating curve of the discriminant, corresponding to no separation.

The procedure is validated by applying it to a signal-depleted region, defined by shifting the signal and control regions according to the definition of χ, using as values of the center position $c_1 = 179\,\mathrm{GeV}$ and $c_2 = 172\,\mathrm{GeV}$. The center of this validation region is chosen to be along the $m_{\mathrm{H}_1} = 1.04\,m_{\mathrm{H}_2}$ line used in the reconstruction of the H candidates to provide an accurate proxy of the analysis region. In analogy to the analysis regions, signal and control validation regions, V_{SR} and V_{CR}, are defined as $\chi < 25\,\mathrm{GeV}$ and $25 \leq \chi < 50\,\mathrm{GeV}$, respectively. After training and applying the reweighting BDT in these regions and computing the normalization transfer factors, the data in V_{SR}^{4b} were found to be compatible within uncertainties with the predicted background, validating the modeling method. The agreement is quantified with a goodness-of-fit test based on a saturated model [61] performed on the observables used in the analysis. For a fit under the background-only hypothesis, a p-value of 53% is observed, ranging between 12 and 83% for the individual categories.

The impact on the estimated background from the presence of signal events in the A_{SR}^{3b} region due to jets failing the b tagging requirement is estimated by generating pseudo-data in A_{SR}^{4b} according to the modeled background plus simulated HH signal, and fitting them under a different background hypothesis that includes the contribution from signal events in A_{SR}^{3b} weighted as done for background events. This study is repeated for signal yields up to five times larger than the expected sensitivity of this search, and in all cases a signal yield compatible with the true one is observed. We conclude that signal events in A_{SR}^{3b} do not have any significant impact on the background model and on the results.

For the background model, systematic uncertainties are considered for the limited number of events in the A_{SR}^{3b}. These uncertainties are uncorrelated across the individual bins of the background templates used for the statistical analysis, and correspond to the propagation of a bin-by-bin Poisson uncertainty from the A_{SR}^{3b} to the A_{SR}^{4b} region. The uncertainty in the estimation of the transfer factor from the 3b to the 4b region is computed from the statistical uncertainty in A_{CR}^{3b} and A_{CR}^{4b} and is 1–2% for the ggF categories, 2-3% for the SM-like VBF category and 18–32% for the anomalous $\kappa_{2\mathrm{V}}$-like VBF category. An uncertainty is also considered for the limited number of events in the validation region, in some cases lower than the number of events in the analysis region. It is large (30–33%) for the anomalous $\kappa_{2\mathrm{V}}$-like VBF category while it is about 2-3% and below 1% for the other VBF category and the ggF categories, respectively, and represents the inherent limitation on the capability to validate the performance of the background model. For analysis categories where the agreement between the observed and predicted background yields in the validation region differs by more than one standard deviation, an additional uncertainty is included and ranges between 1.5 and 4.7%, depending on the category and year. Finally, the uncertainty in the performance of the reweighting method to interpolate the kinematics from A_{CR} into A_{SR} is estimated by performing alternative trainings in two regions of A_{CR}. The two regions are defined by requiring the product of $\mathrm{m}_{\perp}$ and $\mathrm{m}_{\parallel}$ to be either positive or negative, where $\mathrm{m}_{\perp}$ is defined as the projection of the point in the $(m_{\mathrm{H}_1}, m_{\mathrm{H}_2})$ plane onto the axis perpendicular to the one corresponding to $\mathrm{m}_{\parallel}$ previously defined. The two regions correspond to four quadrants in the $(m_{\mathrm{H}_1}, m_{\mathrm{H}_2})$ plane, and allow for tests of the capability of the reweighting method to model A_{SR}, starting from events with kinematic properties that are either similar ($\mathrm{m}_{\perp}\mathrm{m}_{\parallel} < 0$) or that are harder or softer ($\mathrm{m}_{\perp}\mathrm{m}_{\parallel} > 0$) compared to A_{SR}, thus testing the capability of the model to interpolate across different learning domains. The alternative background templates obtained from trainings in these regions represent the uncertainty on the shape of the predicted background distribution. All the uncertainties are independent between the 2016 and 2017–2018 background models. The dominant uncertainties in this search are those associated to the background modeling, and in particular the bin-by-bin and the normalization uncertainties due to the limited number of events in $A^{3\mathrm{b}}_{\mathrm{SR}}$, $A^{3\mathrm{b}}_{\mathrm{CR}}$ and $A^{4\mathrm{b}}_{\mathrm{CR}}$.

The effects of the imperfect modeling of the detector response and the inaccurate simulation of signal processes are accounted for as systematic uncertainties. The most important sources of systematic uncertainty are the total integrated luminosity, the jet energy scale and resolution, the efficiency of the trigger and of the b-tagging requirements, the modeling of the pileup distribution, the $\mathrm{HH} \to \mathrm{b\bar{b}b\bar{b}}$ branching fraction, and the parameters used for the generators. A specific uncertainty on the parton shower is considered for the VBF production mode. Uncertainties on the theoretically determined HH cross section are considered only when quoting a limit on the HH signal strength (μ), defined as the ratio of the value of the cross section limit relative to the theoretical cross section expectation in the SM ($\sigma_{\mathrm{HH}}/\sigma^{\mathrm{SM}}_{\mathrm{HH}}$). These uncertainties are negligible in comparison to the background uncertainties. See Appendix A for more details.

A multivariate BDT discriminant is trained with the XGBOOST software [62] in the two ggF subcategories to separate the signal from the weighted $A^{3\mathrm{b}}_{\mathrm{SR}}$ background events. The discriminant uses as inputs $p_{\mathrm{T}}(\mathrm{H}_1)$, $p_{\mathrm{T}}(\mathrm{H}_2)$, m_{H_1}, m_{H_2}, $|\Delta\eta(\mathrm{H}_1,\mathrm{H}_2)|$, m_{HH}, $p_{\mathrm{T}}(\mathrm{HH})$, $\Delta R^{\mathrm{H}_1}(\mathrm{bb})$, $\Delta R^{\mathrm{H}_2}(\mathrm{bb})$, ΔR^{min}, $|\Delta\eta|^{\mathrm{max}}$, $\sum p_{\mathrm{T}}$, N^T_{b}, $\sum R_e$, $|\cos\theta^*|$, and $|\cos\theta^{\mathrm{H}_1}_{\mathrm{b}}|$. For each subcategory, a separate training is performed to separate the SM ggF HH signal from the weighted $A^{3\mathrm{b}}_{\mathrm{SR}}$ region data. Since the same $A^{3\mathrm{b}}_{\mathrm{SR}}$ data are also used to model the background, this data set is divided in two equal-size subsamples. Two trainings are performed on each half and applied to the other half, and the two partial background templates are added together. In this way, the full data set can be used for the modeling, while the BDT discriminant is not evaluated on events used for its training. In the VBF SM-like category, m_{HH} is used as the discriminating variable, while in the anomalous $\kappa_{2\mathrm{V}}$-like category, a counting experiment is performed because of the small number of expected background events. The distributions of these variables are shown in Fig. 1. For the VBF anomalous $\kappa_{2\mathrm{V}}$-like category in the 2016 (2017–2018) data set, 4 (13) events are observed for a total of 4.0 ± 1.3 (15.0 ± 3.4) background and 1.5 (3.5) VBF $\kappa_{2\mathrm{V}} = 2$ signal events expected.

A binned maximum likelihood fit is simultaneously performed in all analysis categories, where the systematic uncertainties previously discussed are introduced as nuisance parameters. No deviation from a background-only hypothesis is observed. Results are used to set 95% CL upper limits on the HH production cross section using the modified frequentist $\mathrm{CL_s}$ criterion [63, 64] with the profile likelihood ratio modified for upper limits [65] as the test statistics, and making use of the asymptotic approximation [66].

Figure 2 shows the 95% CL cross section upper limits as functions of the κ_λ and $\kappa_{2\mathrm{V}}$ values. The value of κ_λ is observed (expected) to be in the range $-2.3 < \kappa_\lambda < 9.4$ ($-5.0 < \kappa_\lambda < 12.0$) at

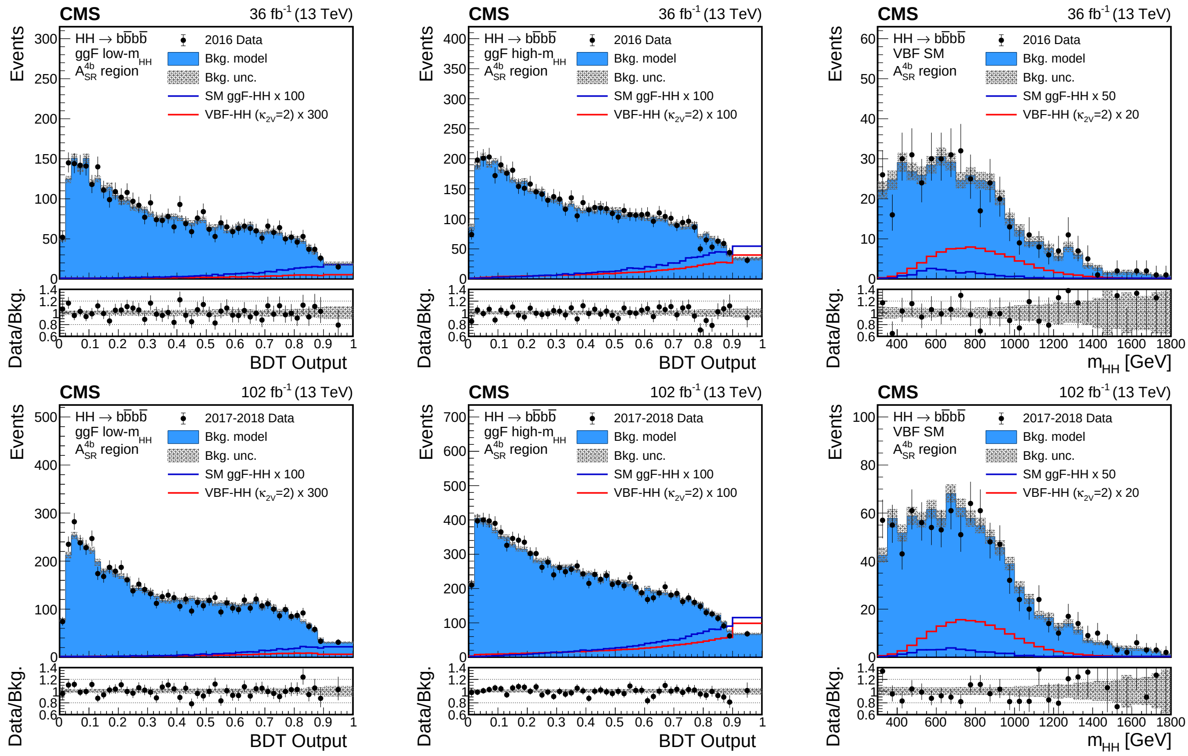

Figure 1: Distributions of the events observed in the A_{SR}^{4b} signal region for 2016 (top) and 2017–2018 (bottom) data. The two leftmost columns show the BDT output in the low- and high-mass categories, and the rightmost column shows the m_{HH} distribution in the VBF SM-like category.

the 95% CL, while the value of κ_{2V} is observed (expected) to be in the range $-0.1 < \kappa_{2V} < 2.2$ ($-0.4 < \kappa_{2V} < 2.5$) at the 95% CL. The total HH production cross section, defined as the sum of the ggF and VBF production modes, is observed (expected) to be smaller than 120 (238) fb, corresponding to 3.9 (7.8) times the SM prediction, when uncertainties on the theoretical production cross section are included. The HH VBF production cross section is observed (expected) to be smaller than 226 (412) times the SM prediction. The deficit in the observed number of events localized around the BDT discriminant values of 0.85–0.9 in the ggF high-mass category in the 2017–2018 data set, which provides the largest sensitivity to the signal, results in the observed limit to be below the expected one. Studies of the background model for the individual BDT input variables and the absence of deficit in the 2016 data in the same high-sensitivity region, and in the other categories suggest that this under fluctuation is of statistical nature.

The intervals containing 68 and 95% of the expected signal strength upper limits correspond to $[5.5, 12.3]$ and $[4.0, 18.7]$ ($[291, 598]$ and $[216, 846]$) for the ggF (VBF) production modes, and the observed limit is thus compatible with the expectation within about two standard deviations. The sensitivity is mostly limited by the number of events in the signal and control regions of the analysis. Tabulated results are available in the HEPData record of this analysis [67].

In summary, a search for the production of Higgs boson pairs via gluon and vector boson fusion in the four b quark decay channel has been presented. The data are found to be statistically compatible with the background-only hypothesis, and an observed (expected) upper limit at the 95% confidence level is set to 3.9 (7.8) times the SM prediction for the combined ggF and VBF HH cross section. The value of the Higgs boson self-coupling, normalized to the SM expectation, is observed (expected) to be in the range $-2.3 < \kappa_\lambda < 9.4$ ($-5.0 < \kappa_\lambda < 12.0$), and the value of the coupling of Higgs boson pairs to vector boson pairs, normalized to the

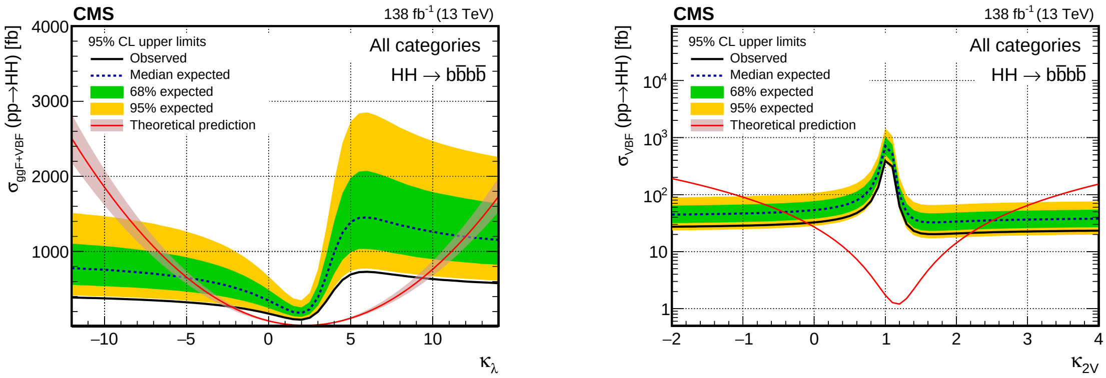

Figure 2: Observed and expected 95% CL upper limits on the $\sigma_{\text{ggF+VBF}}$ HH cross section as a function of κ_λ (left), and on the σ_{VBF} HH cross section as a function of κ_{2V} (right). The green (yellow) band indicates the regions containing 68% (95%) of the limit values expected under the background-only hypothesis. The red lines denote the theoretical cross section expectation assuming that other couplings are set to the SM prediction. For the cross section limit as a function of κ_{2V}, the ggF HH production is assumed to correspond to the SM prediction.

SM expectation, to be in the range $-0.1 < \kappa_{2V} < 2.2$ ($-0.4 < \kappa_{2V} < 2.5$). These are the most stringent observed constraints to date on the HH production cross sections and on the κ_{2V} coupling.

Acknowledgments

We congratulate our colleagues in the CERN accelerator departments for the excellent performance of the LHC and thank the technical and administrative staffs at CERN and at other CMS institutes for their contributions to the success of the CMS effort. In addition, we gratefully acknowledge the computing centers and personnel of the Worldwide LHC Computing Grid and other centers for delivering so effectively the computing infrastructure essential to our analyses. Finally, we acknowledge the enduring support for the construction and operation of the LHC, the CMS detector, and the supporting computing infrastructure provided by the following funding agencies: BMBWF and FWF (Austria); FNRS and FWO (Belgium); CNPq, CAPES, FAPERJ, FAPERGS, and FAPESP (Brazil); MES (Bulgaria); CERN; CAS, MoST, and NSFC (China); MINCIENCIAS (Colombia); MSES and CSF (Croatia); RIF (Cyprus); SENESCYT (Ecuador); MoER, ERC PUT and ERDF (Estonia); Academy of Finland, MEC, and HIP (Finland); CEA and CNRS/IN2P3 (France); BMBF, DFG, and HGF (Germany); GSRT (Greece); NKFIA (Hungary); DAE and DST (India); IPM (Iran); SFI (Ireland); INFN (Italy); MSIP and NRF (Republic of Korea); MES (Latvia); LAS (Lithuania); MOE and UM (Malaysia); BUAP, CINVESTAV, CONACYT, LNS, SEP, and UASLP-FAI (Mexico); MOS (Montenegro); MBIE (New Zealand); PAEC (Pakistan); MSHE and NSC (Poland); FCT (Portugal); JINR (Dubna); MON, RosAtom, RAS, RFBR, and NRC KI (Russia); MESTD (Serbia); SEIDI, CPAN, PCTI, and FEDER (Spain); MOSTR (Sri Lanka); Swiss Funding Agencies (Switzerland); MST (Taipei); ThEPCenter, IPST, STAR, and NSTDA (Thailand); TUBITAK and TAEK (Turkey); NASU (Ukraine); STFC (United Kingdom); DOE and NSF (USA).

References

[1] ATLAS Collaboration, "Observation of a new particle in the search for the Standard

Model Higgs boson with the ATLAS detector at the LHC", *Phys. Lett. B* **716** (2012) 1, doi:10.1016/j.physletb.2012.08.020, arXiv:1207.7214.

[2] CMS Collaboration, "Observation of a new boson at a mass of 125 GeV with the CMS experiment at the LHC", *Phys. Lett. B* **716** (2012) 30, doi:10.1016/j.physletb.2012.08.021, arXiv:1207.7235.

[3] CMS Collaboration, "Observation of a new boson with mass near 125 GeV in pp collisions at $\sqrt{s} = 7$ and 8 TeV", *JHEP* **06** (2013) 081, doi:10.1007/JHEP06(2013)081, arXiv:1303.4571.

[4] F. Englert and R. Brout, "Broken symmetry and the mass of gauge vector mesons", *Phys. Rev. Lett.* **13** (1964) 321, doi:10.1103/PhysRevLett.13.321.

[5] P. W. Higgs, "Broken symmetries and the masses of gauge bosons", *Phys. Rev. Lett.* **13** (1964) 508, doi:10.1103/PhysRevLett.13.508.

[6] G. S. Guralnik, C. R. Hagen, and T. W. B. Kibble, "Global conservation laws and massless particles", *Phys. Rev. Lett.* **13** (1964) 585, doi:10.1103/PhysRevLett.13.585.

[7] S. Dawson, S. Dittmaier, and M. Spira, "Neutral Higgs boson pair production at hadron colliders: QCD corrections", *Phys. Rev. D* **58** (1998) 115012, doi:10.1103/PhysRevD.58.115012, arXiv:hep-ph/9805244.

[8] S. Borowka et al., "Higgs boson pair production in gluon fusion at next-to-leading order with full top-quark mass dependence", *Phys. Rev. Lett.* **117** (2016) 012001, doi:10.1103/PhysRevLett.117.079901, arXiv:1604.06447. [Erratum: doi:10.1103/PhysRevLett.117.079901].

[9] J. Baglio et al., "Gluon fusion into Higgs pairs at NLO QCD and the top mass scheme", *Eur. Phys. J. C* **79** (2019) 459, doi:10.1140/epjc/s10052-019-6973-3, arXiv:1811.05692.

[10] D. de Florian and J. Mazzitelli, "Higgs boson pair production at next-to-next-to-leading order in QCD", *Phys. Rev. Lett.* **111** (2013) 201801, doi:10.1103/PhysRevLett.111.201801, arXiv:1309.6594.

[11] D. Y. Shao, C. S. Li, H. T. Li, and J. Wang, "Threshold resummation effects in Higgs boson pair production at the LHC", *JHEP* **07** (2013) 169, doi:10.1007/JHEP07(2013)169, arXiv:1301.1245.

[12] D. de Florian and J. Mazzitelli, "Higgs pair production at next-to-next-to-leading logarithmic accuracy at the LHC", *JHEP* **09** (2015) 053, doi:10.1007/JHEP09(2015)053, arXiv:1505.07122.

[13] M. Grazzini et al., "Higgs boson pair production at NNLO with top quark mass effects", *JHEP* **05** (2018) 059, doi:10.1007/JHEP05(2018)059, arXiv:1803.02463.

[14] J. Baglio et al., "$gg \to HH$: Combined uncertainties", *Phys. Rev. D* **103** (2021) 056002, doi:10.1103/PhysRevD.103.056002, arXiv:2008.11626.

[15] F. A. Dreyer and A. Karlberg, "Vector-boson fusion Higgs pair production at N^3LO", *Phys. Rev. D* **98** (2018) 114016, doi:10.1103/PhysRevD.98.114016, arXiv:1811.07906.

[16] F. Bishara, R. Contino, and J. Rojo, "Higgs pair production in vector-boson fusion at the LHC and beyond", *Eur. Phys. J. C* **77** (2017) 481, doi:10.1140/epjc/s10052-017-5037-9, arXiv:1611.03860.

[17] ATLAS Collaboration, "Search for pair production of Higgs bosons in the $b\overline{b}b\overline{b}$ final state using proton-proton collisions at $\sqrt{s} = 13$ TeV with the ATLAS detector", *JHEP* **01** (2019) 030, doi:10.1007/JHEP01(2019)030, arXiv:1804.06174.

[18] CMS Collaboration, "Search for nonresonant Higgs boson pair production in the $b\overline{b}b\overline{b}$ final state at $\sqrt{s} = 13$ TeV", *JHEP* **04** (2019) 112, doi:10.1007/JHEP04(2019)112, arXiv:1810.11854.

[19] ATLAS Collaboration, "Search for resonant and non-resonant Higgs boson pair production in the $b\overline{b}\tau^+\tau^-$ decay channel in pp collisions at $\sqrt{s} = 13$ TeV with the ATLAS detector", *Phys. Rev. Lett.* **121** (2018) 191801, doi:10.1103/PhysRevLett.121.191801, arXiv:1808.00336. [Erratum: doi:10.1103/PhysRevLett.122.089901].

[20] CMS Collaboration, "Search for Higgs boson pair production in events with two bottom quarks and two tau leptons in proton-proton collisions at $\sqrt{s}$ = 13 TeV", *Phys. Lett. B* **778** (2018) 101, doi:10.1016/j.physletb.2018.01.001, arXiv:1707.02909.

[21] ATLAS Collaboration, "Search for Higgs boson pair production in the $b\overline{b}WW^*$ decay mode at $\sqrt{s} = 13$ TeV with the ATLAS detector", *JHEP* **04** (2019) 092, doi:10.1007/JHEP04(2019)092, arXiv:1811.04671.

[22] CMS Collaboration, "Search for resonant and nonresonant Higgs boson pair production in the $b\overline{b}\ell\nu\ell\nu$ final state in proton-proton collisions at $\sqrt{s} = 13$ TeV", *JHEP* **01** (2018) 054, doi:10.1007/JHEP01(2018)054, arXiv:1708.04188.

[23] ATLAS Collaboration, "Search for Higgs boson pair production in the $\gamma\gamma b\overline{b}$ final state with 13 TeV pp collision data collected by the ATLAS experiment", *JHEP* **11** (2018) 040, doi:10.1007/JHEP11(2018)040, arXiv:1807.04873.

[24] CMS Collaboration, "Search for Higgs boson pair production in the $\gamma\gamma b\overline{b}$ final state in pp collisions at $\sqrt{s} = 13$ TeV", *Phys. Lett. B* **788** (2019) 7, doi:10.1016/j.physletb.2018.10.056, arXiv:1806.00408.

[25] ATLAS Collaboration, "Search for Higgs boson pair production in the $\gamma\gamma WW^*$ channel using pp collision data recorded at $\sqrt{s} = 13$ TeV with the ATLAS detector", *Eur. Phys. J. C* **78** (2018) 1007, doi:10.1140/epjc/s10052-018-6457-x, arXiv:1807.08567.

[26] ATLAS Collaboration, "Search for Higgs boson pair production in the $WW^{(*)}WW^{(*)}$ decay channel using ATLAS data recorded at $\sqrt{s} = 13$ TeV", *JHEP* **05** (2019) 124, doi:10.1007/JHEP05(2019)124, arXiv:1811.11028.

[27] ATLAS Collaboration, "Combination of searches for Higgs boson pairs in pp collisions at $\sqrt{s}$ =13 TeV with the ATLAS detector", *Phys. Lett. B* **800** (2020) 135103, doi:10.1016/j.physletb.2019.135103, arXiv:1906.02025.

[28] CMS Collaboration, "Combination of searches for Higgs boson pair production in proton-proton collisions at $\sqrt{s} = 13$ TeV", *Phys. Rev. Lett.* **122** (2019) 121803, doi:10.1103/PhysRevLett.122.121803, arXiv:1811.09689.

[29] ATLAS Collaboration, "Search for non-resonant Higgs boson pair production in the $b\overline{b}\ell\nu\ell\nu$ final state with the ATLAS detector in pp collisions at $\sqrt{s} = 13$ TeV", *Phys. Lett. B* **801** (2020) 135145, doi:10.1016/j.physletb.2019.135145, arXiv:1908.06765.

[30] CMS Collaboration, "Search for nonresonant Higgs boson pair production in final states with two bottom quarks and two photons in proton-proton collisions at $\sqrt{s}$ = 13 TeV", *JHEP* **03** (2021) 257, doi:10.1007/JHEP03(2021)257, arXiv:2011.12373.

[31] ATLAS Collaboration, "Search for Higgs boson pair production in the two bottom quarks plus two photons final state in pp collisions at $\sqrt{s} = 13$ TeV with the ATLAS detector", 2021. arXiv:2112.11876. Submitted to PRD.

[32] ATLAS Collaboration, "Search for the HH $\rightarrow b\overline{b}b\overline{b}$ process via vector-boson fusion production using proton-proton collisions at $\sqrt{s} = 13$ TeV with the ATLAS detector", *JHEP* **07** (2020) 108, doi:10.1007/JHEP07(2020)108, arXiv:2001.05178.

[33] LHC Higgs Cross Section Working Group, "Handbook of LHC Higgs cross sections: 4. Deciphering the nature of the Higgs sector", *CERN* (2016) doi:10.23731/CYRM-2017-002, arXiv:1610.07922.

[34] CMS Collaboration, "The CMS experiment at the CERN LHC", *JINST* **3** (2008) S08004, doi:10.1088/1748-0221/3/08/S08004.

[35] CMS Collaboration, "Performance of the CMS Level-1 trigger in proton-proton collisions at $\sqrt{s} = 13$ TeV", *JINST* **15** (2020) P10017, doi:10.1088/1748-0221/15/10/P10017, arXiv:2006.10165.

[36] CMS Collaboration, "The CMS trigger system", *JINST* **12** (2017) P01020, doi:10.1088/1748-0221/12/01/P01020, arXiv:1609.02366.

[37] CMS Collaboration, "Performance of electron reconstruction and selection with the CMS detector in proton-proton collisions at $\sqrt{s} = 8$ TeV", *JINST* **10** (2015) P06005, doi:10.1088/1748-0221/10/06/P06005, arXiv:1502.02701.

[38] CMS Collaboration, "Electron and photon reconstruction and identification with the CMS experiment at the CERN LHC", *JINST* **16** (2021) P05014, doi:10.1088/1748-0221/16/05/P05014, arXiv:2012.06888.

[39] CMS Collaboration, "Performance of the CMS muon detector and muon reconstruction with proton-proton collisions at $\sqrt{s} = 13$ TeV", *JINST* **13** (2018) P06015, doi:10.1088/1748-0221/13/06/P06015, arXiv:1804.04528.

[40] CMS Collaboration, "Performance of photon reconstruction and identification with the CMS Detector in proton-proton collisions at $\sqrt{s}$ = 8 TeV", *JINST* **10** (2015) P08010, doi:10.1088/1748-0221/10/08/P08010, arXiv:1502.02702.

[41] CMS Collaboration, "Description and performance of track and primary-vertex reconstruction with the CMS tracker", *JINST* **9** (2014) P10009, doi:10.1088/1748-0221/9/10/P10009, arXiv:1405.6569.

[42] CMS Collaboration, "Particle-flow reconstruction and global event description with the CMS detector", *JINST* **12** (2017) P10003, doi:10.1088/1748-0221/12/10/P10003, arXiv:1706.04965.

[43] CMS Collaboration, “Performance of reconstruction and identification of τ leptons decaying to hadrons and ν_τ in pp collisions at $\sqrt{s} = 13$ TeV”, *JINST* **13** (2018) P10005, doi:10.1088/1748-0221/13/10/P10005, arXiv:1809.02816.

[44] CMS Collaboration, “Jet energy scale and resolution in the CMS experiment in pp collisions at 8 TeV”, *JINST* **12** (2017) P02014, doi:10.1088/1748-0221/12/02/P02014, arXiv:1607.03663.

[45] CMS Collaboration, “Performance of missing transverse momentum reconstruction in proton-proton collisions at $\sqrt{s} = 13$ TeV using the CMS detector”, *JINST* **14** (2019) P07004, doi:10.1088/1748-0221/14/07/P07004, arXiv:1903.06078.

[46] M. Cacciari, G. P. Salam, and G. Soyez, “The anti-k_T jet clustering algorithm”, *JHEP* **04** (2008) 063, doi:10.1088/1126-6708/2008/04/063, arXiv:0802.1189.

[47] M. Cacciari, G. P. Salam, and G. Soyez, “FastJet user manual”, *Eur. Phys. J. C* **72** (2012) 1896, doi:10.1140/epjc/s10052-012-1896-2, arXiv:1111.6097.

[48] CMS Collaboration, “Identification of heavy-flavour jets with the CMS detector in pp collisions at 13 TeV”, *JINST* **13** (2018) P05011, doi:10.1088/1748-0221/13/05/P05011, arXiv:1712.07158.

[49] E. Bols et al., “Jet flavour classification using DeepJet”, *JINST* **15** (2020) P12012, doi:10.1088/1748-0221/15/12/P12012, arXiv:2008.10519.

[50] S. Alioli, P. Nason, C. Oleari, and E. Re, “NLO vector-boson production matched with shower in POWHEG”, *JHEP* **07** (2008) 060, doi:10.1088/1126-6708/2008/07/060, arXiv:0805.4802.

[51] P. Nason, “A New method for combining NLO QCD with shower Monte Carlo algorithms”, *JHEP* **11** (2004) 040, doi:10.1088/1126-6708/2004/11/040, arXiv:hep-ph/0409146.

[52] S. Frixione, P. Nason, and C. Oleari, “Matching NLO QCD computations with Parton Shower simulations: the POWHEG method”, *JHEP* **11** (2007) 070, doi:10.1088/1126-6708/2007/11/070, arXiv:0709.2092.

[53] J. Alwall et al., “The automated computation of tree-level and next-to-leading order differential cross sections, and their matching to parton shower simulations”, *JHEP* **07** (2014) 079, doi:10.1007/JHEP07(2014)079, arXiv:1405.0301.

[54] G. Heinrich et al., “Probing the trilinear Higgs boson coupling in di-Higgs production at NLO QCD including parton shower effects”, *JHEP* **06** (2019) 066, doi:10.1007/JHEP06(2019)066, arXiv:1903.08137.

[55] T. Sjöstrand et al., “An introduction to PYTHIA 8.2”, *Comput. Phys. Commun.* **191** (2015) 159, doi:10.1016/j.cpc.2015.01.024, arXiv:1410.3012.

[56] GEANT4 Collaboration, “GEANT4–a simulation toolkit”, *Nucl. Instrum. Meth. A* **506** (2003) 250, doi:10.1016/S0168-9002(03)01368-8.

[57] CMS Collaboration, “Pileup mitigation at CMS in 13 TeV data”, *JINST* **15** (2020) P09018, doi:10.1088/1748-0221/15/09/P09018, arXiv:2003.00503.

[58] CMS Collaboration, "Jet algorithms performance in 13 TeV data", CMS Physics Analysis Summary CMS-PAS-JME-16-003, CERN, 2017.

[59] CMS Collaboration, "A deep neural network for simultaneous estimation of b jet energy and resolution", *Comput. Softw. Big Sci.* **4** (2020) 10, `doi:10.1007/s41781-020-00041-z`, `arXiv:1912.06046`.

[60] A. Rogozhnikov, "Reweighting with boosted decision trees", *J. Phys. Conf. Ser.* **762** (2016) 012036, `doi:10.1088/1742-6596/762/1/012036`, `arXiv:1608.05806`.

[61] S. Baker and R. D. Cousins, "Clarification of the use of chi-square and likelihood functions in fits to histograms", *Nucl. Instrum. Meth.* **221** (1984) 437, `doi:10.1016/0167-5087(84)90016-4`.

[62] T. Chen and C. Guestrin, "XGBoost: A scalable tree boosting system", in *Proceedings of the 22nd ACM SIGKDD International Conference on Knowledge Discovery and Data Mining*, KDD '16, p. 785. ACM, New York, NY, USA, 2016. `doi:10.1145/2939672.2939785`.

[63] T. Junk, "Confidence level computation for combining searches with small statistics", *Nucl. Instrum. Meth. A* **434** (1999) 435, `doi:10.1016/S0168-9002(99)00498-2`, `arXiv:hep-ex/9902006`.

[64] A. L. Read, "Presentation of search results: the CL_s technique", *J. Phys. G* **28** (2002) 2693, `doi:10.1088/0954-3899/28/10/313`.

[65] The ATLAS Collaboration, The CMS Collaboration, The LHC Higgs Combination Group, "Procedure for the LHC Higgs boson search combination in Summer 2011", Technical Report CMS-NOTE-2011-005, ATL-PHYS-PUB-2011-11, 2011.

[66] G. Cowan, K. Cranmer, E. Gross, and O. Vitells, "Asymptotic formulae for likelihood-based tests of new physics", *Eur. Phys. J. C* **71** (2011) 1554, `doi:10.1140/epjc/s10052-011-1554-0`, `arXiv:1007.1727`. [Erratum: `doi:10.1140/epjc/s10052-013-2501-z`].

[67] "HEPData record for this analysis", 2022. `doi:10.17182/hepdata.114358`.

[68] A. Carvalho et al., "Higgs pair production: choosing benchmarks with cluster analysis", *JHEP* **04** (2016) 126, `doi:10.1007/JHEP04(2016)126`, `arXiv:1507.02245`.

[69] G. Buchalla et al., "Higgs boson pair production in non-linear effective field theory with full m_t-dependence at NLO QCD", *JHEP* **09** (2018) 057, `doi:10.1007/JHEP09(2018)057`, `arXiv:1806.05162`.

[70] J. Alwall et al., "Comparative study of various algorithms for the merging of parton showers and matrix elements in hadronic collisions", *Eur. Phys. J. C* **53** (2008) 473, `doi:10.1140/epjc/s10052-007-0490-5`, `arXiv:0706.2569`.

[71] M. Czakon and A. Mitov, "Top++: A program for the calculation of the top-pair cross-section at hadron colliders", *Comput. Phys. Commun.* **185** (2014) 2930, `doi:10.1016/j.cpc.2014.06.021`, `arXiv:1112.5675`.

[72] R. Frederix and S. Frixione, "Merging meets matching in MC@NLO", *JHEP* **12** (2012) 061, `doi:10.1007/JHEP12(2012)061`, `arXiv:1209.6215`.

[73] J. M. Campbell, R. K. Ellis, and C. Williams, "Vector boson pair production at the LHC", *JHEP* **07** (2011) 018, doi:10.1007/JHEP07(2011)018, arXiv:1105.0020.

[74] CMS Collaboration, "Event generator tunes obtained from underlying event and multiparton scattering measurements", *Eur. Phys. J. C* **76** (2016) 155, doi:10.1140/epjc/s10052-016-3988-x, arXiv:1512.00815.

[75] CMS Collaboration, "Extraction and validation of a new set of CMS PYTHIA8 tunes from underlying-event measurements", *Eur. Phys. J. C* **80** (2020) 4, doi:10.1140/epjc/s10052-019-7499-4, arXiv:1903.12179.

[76] NNPDF Collaboration, "Parton distributions for the LHC Run II", *JHEP* **04** (2015) 040, doi:10.1007/JHEP04(2015)040, arXiv:1410.8849.

[77] NNPDF Collaboration, "Parton distributions from high-precision collider data", *Eur. Phys. J. C* **77** (2017) 663, doi:10.1140/epjc/s10052-017-5199-5, arXiv:1706.00428.

[78] CMS Collaboration, "Precision luminosity measurement in proton-proton collisions at $\sqrt{s} = 13$ TeV in 2015 and 2016 at CMS", 2021. arXiv:2104.01927. Submitted to *Eur. Phys. J. C*.

[79] CMS Collaboration, "CMS luminosity measurement for the 2017 data-taking period at $\sqrt{s} = 13$ TeV", CMS Physics Analysis Summary CMS-PAS-LUM-17-004, CERN, Geneva, 2018.

[80] CMS Collaboration, "CMS luminosity measurement for the 2018 data-taking period at $\sqrt{s} = 13$ TeV", CMS Physics Analysis Summary CMS-PAS-LUM-18-002, CERN, Geneva, 2019.

[81] B. Jäger et al., "Parton-shower effects in Higgs production via vector-boson fusion", *Eur. Phys. J. C* **80** (2020) 756, doi:10.1140/epjc/s10052-020-8326-7, arXiv:2003.12435.

A Simulation details, signal systematic uncertainties, and additional figures

Signal processes from ggF HH production are simulated at NLO accuracy in QCD with POWHEG 2.0 for κ_λ values of 1, 2.45, and 5. Samples for VBF HH production are generated at LO accuracy in QCD using MADGRAPH5_aMC@NLO 2.6.5 for six different sets of $(\kappa_V, \kappa_{2V}, \kappa_\lambda)$ couplings corresponding to $(1, 1, \{0, 1, 2\})$, $(1, \{0, 2\}, 1)$, and $(1.5, 1, 1)$, where each number inside brackets corresponds to one alternative choice that defines one set.

QCD multijet processes are generated with MADGRAPH5_aMC@NLO at LO with MLM merging [70]. The production of pairs of top quarks is simulated at NLO with POWHEG, and normalized to the theoretical cross section at NNLO precision in QCD, including resummation of NNLL soft gluon terms [71]. The production of pairs of Z bosons decaying to hadrons with up to one jet emitted at the matrix element level is simulated with MADGRAPH5_aMC@NLO at NLO with FxFx merging [72] and normalized to the cross section at the same precision [73].

For all simulations, the generators are interfaced with PYTHIA 8.226 (2016) and 8.230 (2017–2018) [55] for parton showering, fragmentation, and modeling of the underlying event using the CUETP8M1 tune for 2016 and the CP5 tune for 2017–2018 [74, 75]. The NNPDF3.0 NLO [76] and NNPDF3.1 NNLO [77] parton distribution function (PDF) sets are used for the 2016 and 2017–2018 samples, respectively. The CMS detector response is modeled with GEANT4 [56].

The total 2016–2018 integrated luminosity has an uncertainty of 1.6%, partially correlated for the three years [78–80]. The uncertainty on the jet energy scale and resolution is accounted for by modifying the corresponding jet properties within the uncertainties associated to their independent measurement, and affects the shape of the signal distributions and the associated yields by up to 5%, partially correlated for the three years. The trigger efficiency in data is measured in an orthogonal data set enriched in multijet $t\bar{t}$ events and compared to the same efficiency obtained from the simulation to derive a correction for the simulated signal events that depends on H_T and on the p_T and DEEPJET discriminant of the selected jets. The uncertainties of these measurements are considered as shape and normalization systematic uncertainties, uncorrelated for the three years, and range between 5 and 40% depending on the coupling and the category, with the largest values for the low-mass ggF category in regions of the phase space with little separation from the background. The impact of this uncertainty on the sensitivity is of about 1%. The b-tagging efficiency and the distribution of the DEEPJET discriminant are measured in $t\bar{t}$ and QCD multijet events, and independent uncertainties in this measurement for each year are propagated to the simulated events and range between 5 and 12%. For data recorded in 2016 and 2017, a gradual shift in the timing of the inputs of the ECAL Level-1 trigger in the forward endcap region ($|\eta| > 2.4$) led to an inefficiency whose impact is evaluated using an unbiased data sample, and an uncertainty of 1–2% on the corresponding correction is applied. The uncertainty associated with the correction of the pileup distribution is considered in the analysis by varying the assumed interaction cross section by 4.6%. Uncertainties arising from the theoretical modeling of the signal and related to the factorization and renormalization scales (2–8%), PDF (1–12%), and parton shower parameters (6–13%) used for the sample generation are considered. For the VBF production mode, two alternative models of signal generation that enable and disable a dipole-ordered parton shower in PYTHIA [81] are compared and their difference in the predicted number of signal events ranges from 2 to 13% and is considered to be a systematic uncertainty. Uncertainties in the $HH \to b\bar{b}b\bar{b}$ branching fraction and, when quoting a limit relative to the standard model prediction, theoretical uncertainties on the total HH cross section prediction are also considered.

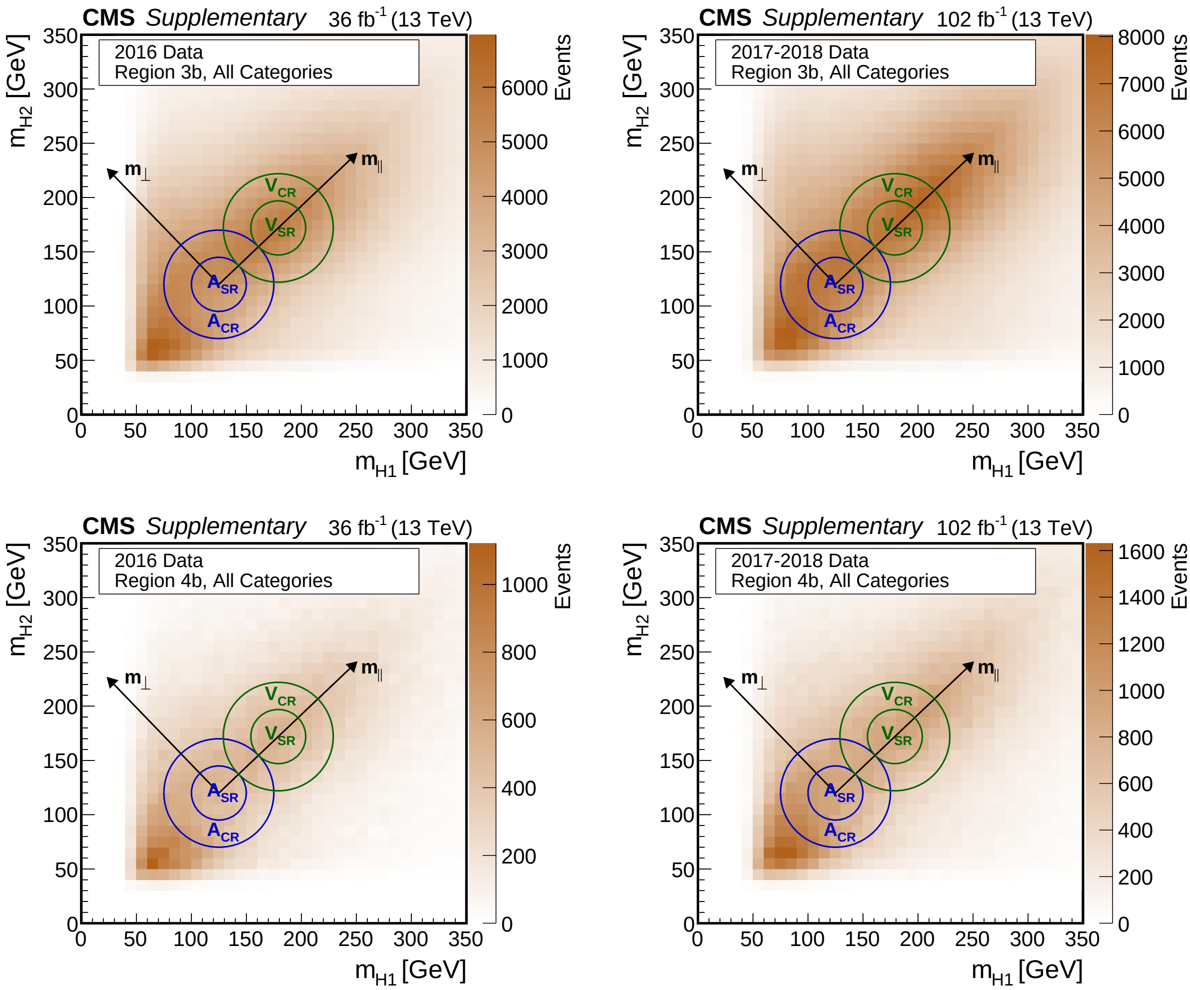

Figure A.1: Distribution of data events selected in the three (top row) and four (bottom row) b-tagged jet categories for events recorded in 2016 (left column) and 2017 and 2018 (right column) as a function of the masses of the two Higgs boson candidates. The blue and green circles correspond to the analysis and validation regions, respectively, denoted by the letters A and V. The inner circle corresponds to the signal region while the ring around it defines the control region used for the background modeling. The figure also shows the definition of the variables $m_{\parallel}$ and $m_{\perp}$ that are used in the analysis.

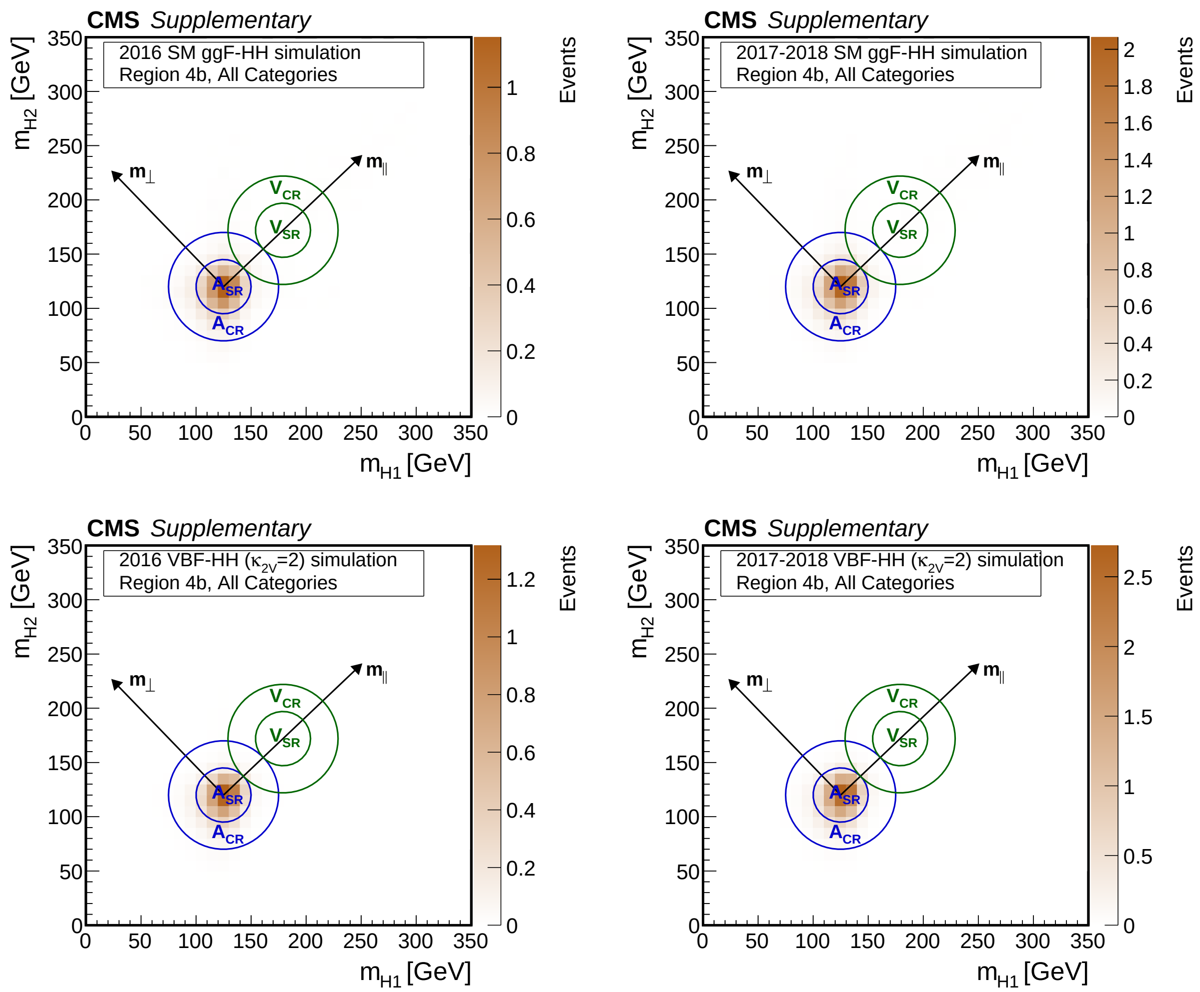

Figure A.2: Distribution of simulated signal events selected for the SM ggF production (top row) and $\kappa_{2V} = 2$ VBF production (bottom row) as a function of the two Higgs boson candidates masses. The simulations correspond to the events expected for the 2016 data taking (left column) and 2017 and 2018 (right column). The blue and green circles correspond to the analysis and validation regions, respectively, denoted by the letters A and V. The inner circle corresponds to the signal region while the ring around it defines the control region used for the background modeling. The figure also shows the definition of the variables $m_{||}$ and $m_{\perp}$ that are used in the analysis.

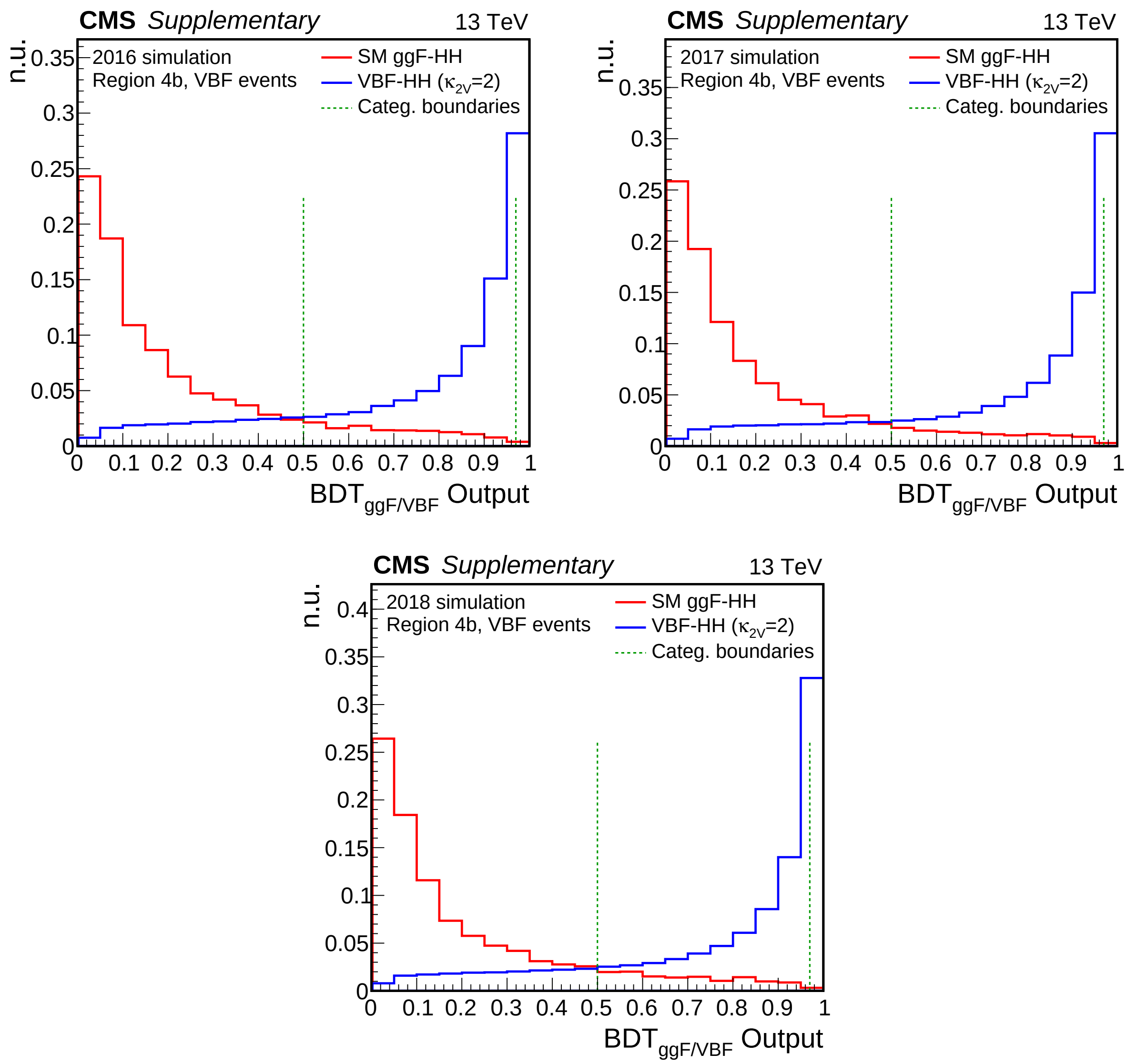

Figure A.3: Distribution of the output of the production mode BDT discriminant that is trained to separate the ggF and the VBF production modes, shown for the simulation of the signal processes under the 2016, 2017, and 2018 data taking conditions. The vertical green lines denote the thresholds used for the categorization. Events with a score below 0.5 are classified in the ggF category. Events with a score between 0.5 and 0.97 are classified in the VBF SM-like category. Events with a score above 0.97 are classified in the VBF anomalous κ_{2V}-like category.

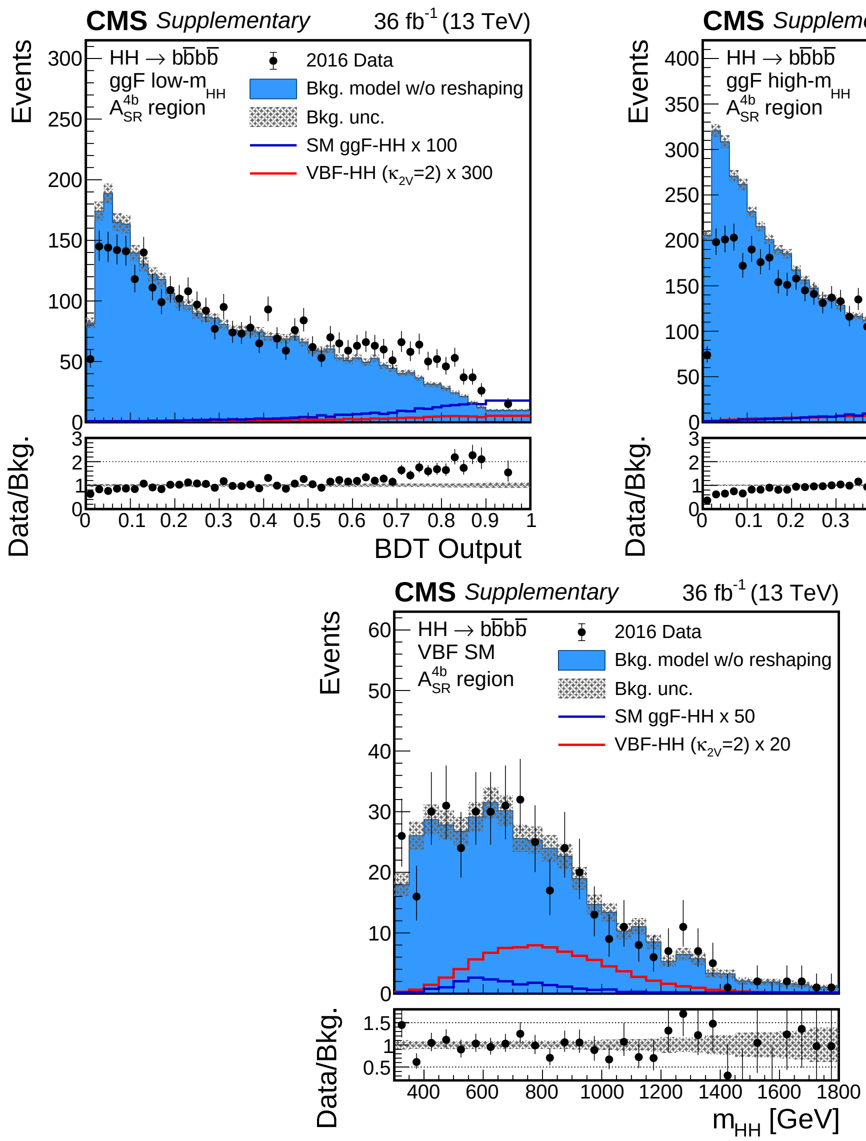

Figure A.4: Prediction of the background distribution obtained directly from the A^{3b}_{SR} region without the application of the BDT reweighting correction. The top and bottom row show the ggF and VBF categories, respectively, and the data correspond to the 2016 dataset. For the former, the output of the BDT discriminant is shown for the low-mass category on the left and for the high-mass category on the right. For the latter, the m_{HH} distribution in the SM-like category is shown. The anomalous κ_{2V}-like category is not shown because no shape correction is applied for it since the overall number of observed events is used to perform a counting experiment. Data are represented by points with error bars, while the ggF (VBF) signal contribution is shown in blue (red) and not stacked. The background prediction without the shape correction is represented by the shaded blue histograms with the associated systematic uncertainties (gray dashed areas).

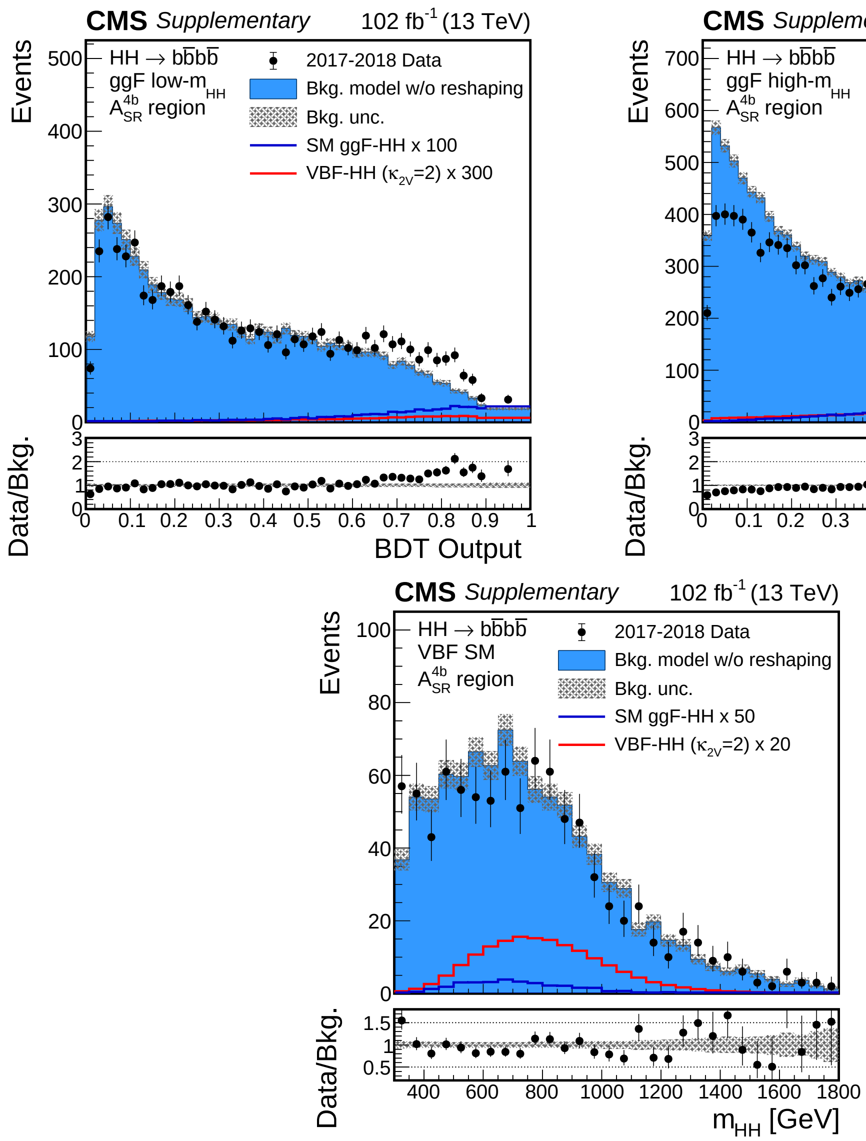

Figure A.5: Prediction of the background distribution obtained directly from the A^{3b}_{SR} region without the application of the BDT reweighting correction. The top and bottom row show the ggF and VBF categories, respectively, and the data correspond to the 2017 and 2018 datasets. For the former, the output of the BDT discriminant is shown for the low-mass category on the left and for the high-mass category on the right. For the latter, the m_{HH} distribution in the SM-like category is shown. The anomalous κ_{2V}-like category is not shown because no shape correction is applied for it since the overall number of observed events is used to perform a counting experiment. Data are represented by points with error bars, while the ggF (VBF) signal contribution is shown in blue (red) and not stacked. The background prediction without the shape correction is represented by the shaded blue histograms with the associated systematic uncertainties (gray dashed areas).

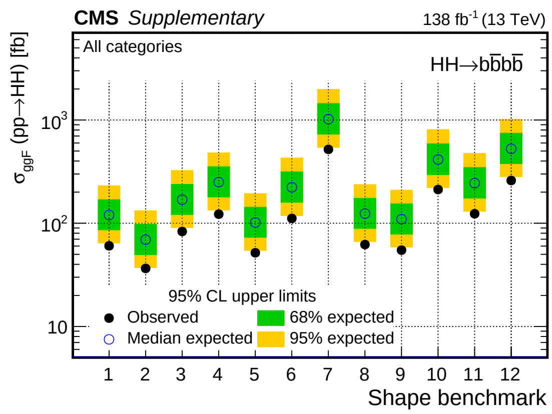

Figure A.6: Observed and expected 95% CL upper limits on the gluon fusion Higgs boson pair production cross section for different combinations of Higgs boson couplings in the effective Lagrangian parametrization. The numbers from 1 to 12 denote the shape benchmarks defined in Ref. [68], corresponding to points in the five-dimensional parameter space with characteristic kinematic properties of the HH system. The leading order simulation is reweighted to match the m_{HH} spectrum at the next-to-leading order as predicted by simulation described in Ref. [69]. The inner (green) band and the outer (yellow) band indicate the regions containing 68 and 95%, respectively, of the distribution of limits expected under the background-only hypothesis.

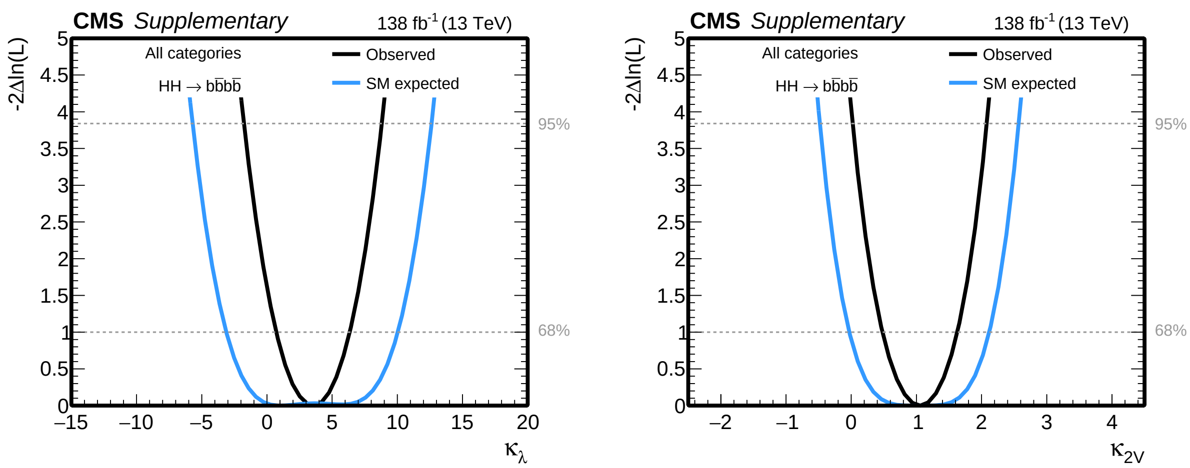

Figure A.7: Expected and observed likelihood scan as a function of the κ_λ (left) and κ_{2V} (right) couplings. All the couplings that are not displayed in the figure are fixed to their SM prediction.

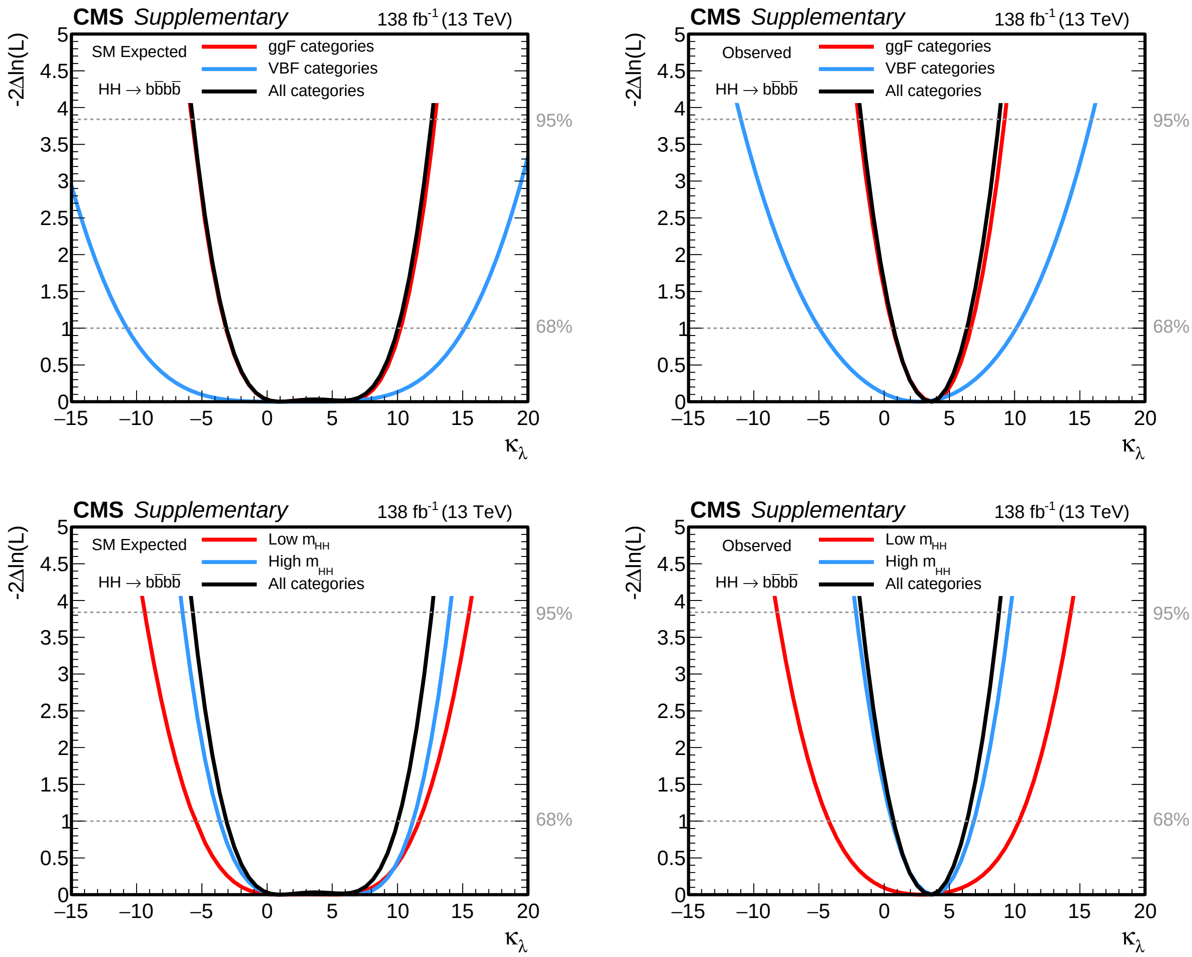

Figure A.8: Expected (left column) and observed (right column) likelihood scans as a function of the κ_λ couplings, assuming all the other couplings to be fixed to their SM prediction. The top row shows the contribution of the ggF (red) and VBF (blue) categories and their combination (black). The bottom row shows the contribution of the low- (red) and high-mass (blue) ggF categories, and the overall combination of all the ggF and VBF categories (black). For all the curves, the 2016, 2017 and 2018 datasets are combined.

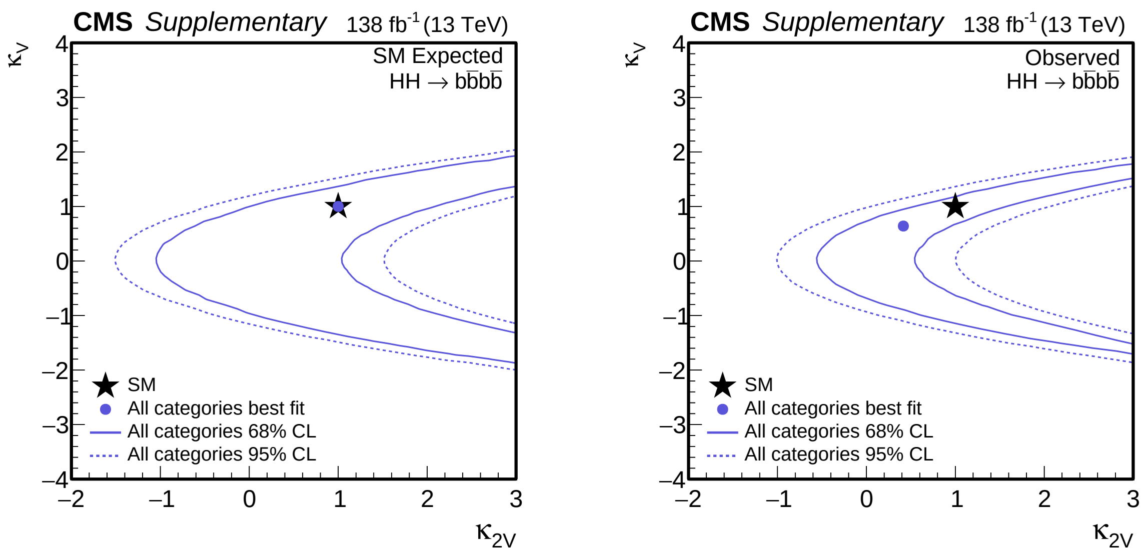

Figure A.9: Expected (left) and observed (right) regions allowed at the 68 and 95% CL as a function of the κ_{2V} and κ_{V} couplings, assuming the κ_{t} and κ_{λ} couplings to be fixed to 1. The dot denotes the best-fit hypothesis while the star marker represents the SM prediction.

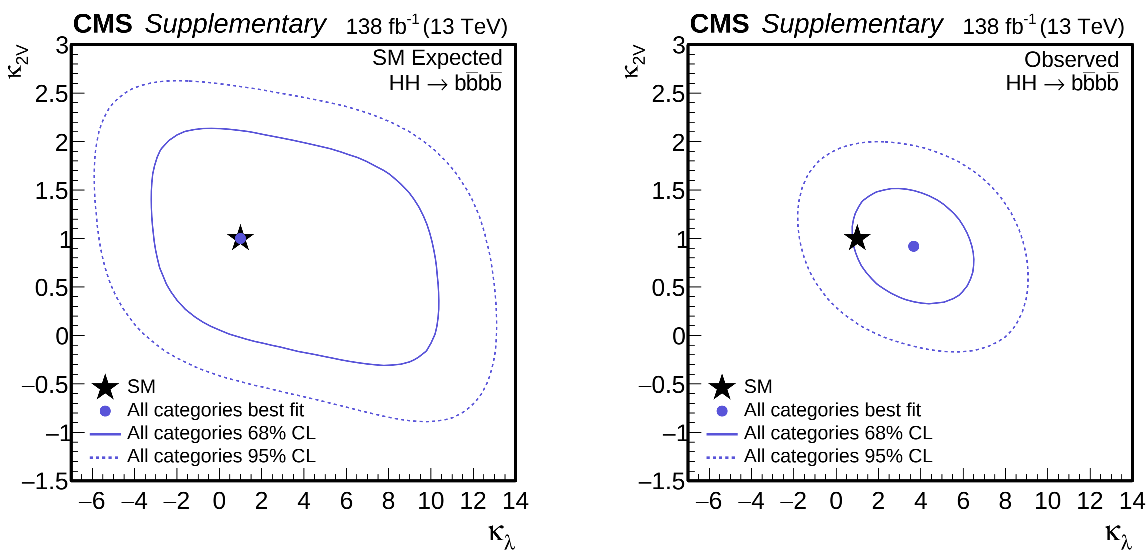

Figure A.10: Expected (left) and observed (right) regions allowed at the 68 and 95% CL as a function of the κ_{2V} and κ_{λ} couplings, assuming the κ_{t} and κ_{V} couplings to be fixed to 1. The dot denotes the best-fit hypothesis while the star marker represents the SM prediction.

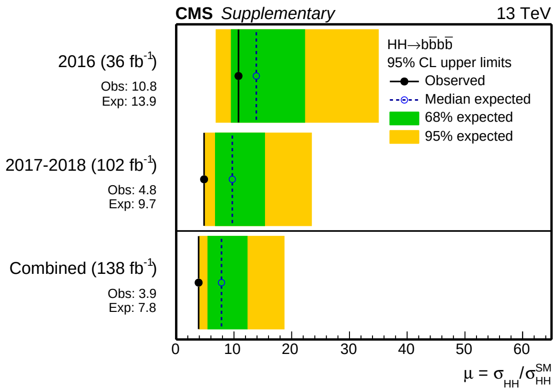

Figure A.11: Observed and expected 95% CL limits on the standard model Higgs boson pair (HH) production signal strength (μ) by year: 2016 (top row), 2017-2018 (center row) and Combined (bottom row).

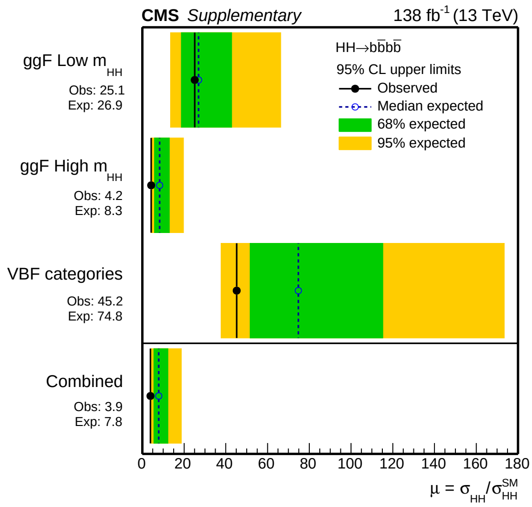

Figure A.12: Observed and expected 95% CL limits on the standard model Higgs boson pair (HH) production signal strength (μ) by category: ggF Low m_{HH} (first row), ggF High m_{HH} (second row), VBF categories (third row), and Combined (fourth row).

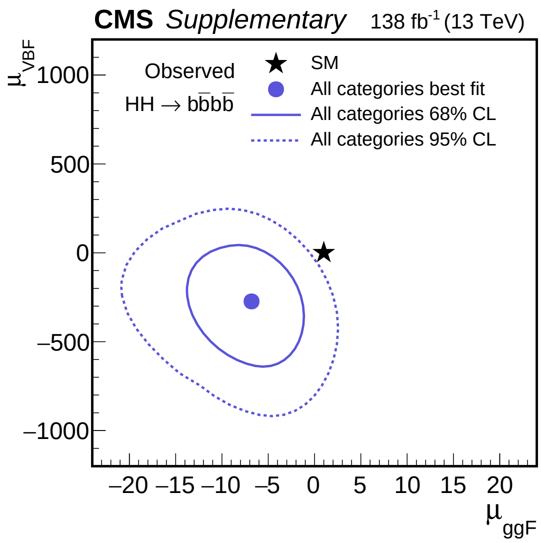

Figure A.13: Signal strength of the SM ggF and VBF production modes. The solid (dashed) line denotes the contour corresponding to the 68% (95%) confidence levels. The circle represents the best-fit point while the star marker represents the SM expectation. The signal strength is treated as a free parameter that is not bound to be positive, and the best-fit point takes a negative value as a consequence of the deficit in the observed number of the events discussed in the Letter.

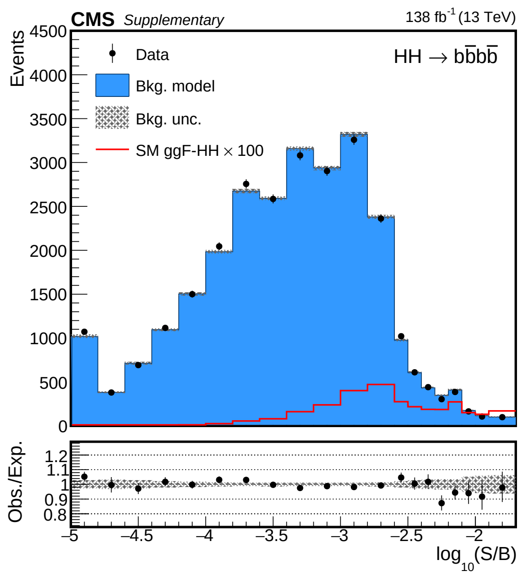

Figure A.14: Distribution of the ratio of the expected signal to background ratio for events selected in the categories of the analysis. The leftmost bin also includes events that are below the represented x-axis range.

B The CMS Collaboration

Yerevan Physics Institute, Yerevan, Armenia
A. Tumasyan

Institut für Hochenergiephysik, Vienna, Austria
W. Adam, J.W. Andrejkovic, T. Bergauer, S. Chatterjee, K. Damanakis, M. Dragicevic, A. Escalante Del Valle, R. Frühwirth[1], M. Jeitler[1], N. Krammer, L. Lechner, D. Liko, I. Mikulec, P. Paulitsch, F.M. Pitters, J. Schieck[1], R. Schöfbeck, D. Schwarz, S. Templ, W. Waltenberger, C.-E. Wulz[1]

Institute for Nuclear Problems, Minsk, Belarus
V. Chekhovsky, A. Litomin, V. Makarenko

Universiteit Antwerpen, Antwerpen, Belgium
M.R. Darwish[2], E.A. De Wolf, T. Janssen, T. Kello[3], A. Lelek, H. Rejeb Sfar, P. Van Mechelen, S. Van Putte, N. Van Remortel

Vrije Universiteit Brussel, Brussel, Belgium
F. Blekman, E.S. Bols, J. D'Hondt, M. Delcourt, H. El Faham, S. Lowette, S. Moortgat, A. Morton, D. Müller, A.R. Sahasransu, S. Tavernier, W. Van Doninck

Université Libre de Bruxelles, Bruxelles, Belgium
D. Beghin, B. Bilin, B. Clerbaux, G. De Lentdecker, L. Favart, A. Grebenyuk, A.K. Kalsi, K. Lee, M. Mahdavikhorrami, I. Makarenko, L. Moureaux, L. Pétré, A. Popov, N. Postiau, E. Starling, L. Thomas, M. Vanden Bemden, C. Vander Velde, P. Vanlaer

Ghent University, Ghent, Belgium
T. Cornelis, D. Dobur, J. Knolle, L. Lambrecht, G. Mestdach, M. Niedziela, C. Roskas, A. Samalan, K. Skovpen, M. Tytgat, B. Vermassen, L. Wezenbeek

Université Catholique de Louvain, Louvain-la-Neuve, Belgium
A. Benecke, A. Bethani, G. Bruno, F. Bury, C. Caputo, P. David, C. Delaere, I.S. Donertas, A. Giammanco, K. Jaffel, Sa. Jain, V. Lemaitre, K. Mondal, J. Prisciandaro, A. Taliercio, M. Teklishyn, T.T. Tran, P. Vischia, S. Wertz

Centro Brasileiro de Pesquisas Fisicas, Rio de Janeiro, Brazil
G.A. Alves, C. Hensel, A. Moraes, P. Rebello Teles

Universidade do Estado do Rio de Janeiro, Rio de Janeiro, Brazil
W.L. Aldá Júnior, M. Alves Gallo Pereira, M. Barroso Ferreira Filho, H. Brandao Malbouisson, W. Carvalho, J. Chinellato[4], E.M. Da Costa, G.G. Da Silveira[5], D. De Jesus Damiao, S. Fonseca De Souza, C. Mora Herrera, K. Mota Amarilo, L. Mundim, H. Nogima, A. Santoro, S.M. Silva Do Amaral, A. Sznajder, M. Thiel, F. Torres Da Silva De Araujo[6], A. Vilela Pereira

Universidade Estadual Paulista (a), Universidade Federal do ABC (b), São Paulo, Brazil
C.A. Bernardes[5], L. Calligaris, T.R. Fernandez Perez Tomei, E.M. Gregores, D.S. Lemos, P.G. Mercadante, S.F. Novaes, Sandra S. Padula

Institute for Nuclear Research and Nuclear Energy, Bulgarian Academy of Sciences, Sofia, Bulgaria
A. Aleksandrov, G. Antchev, R. Hadjiiska, P. Iaydjiev, M. Misheva, M. Rodozov, M. Shopova, G. Sultanov

University of Sofia, Sofia, Bulgaria
A. Dimitrov, T. Ivanov, L. Litov, B. Pavlov, P. Petkov, A. Petrov

Beihang University, Beijing, China
T. Cheng, T. Javaid[7], M. Mittal, L. Yuan

Department of Physics, Tsinghua University, Beijing, China
M. Ahmad, G. Bauer, C. Dozen[8], Z. Hu, J. Martins[9], Y. Wang, K. Yi[10,11]

Institute of High Energy Physics, Beijing, China
E. Chapon, G.M. Chen[7], H.S. Chen[7], M. Chen, F. Iemmi, A. Kapoor, D. Leggat, H. Liao, Z.-A. Liu[7], V. Milosevic, F. Monti, R. Sharma, J. Tao, J. Thomas-Wilsker, J. Wang, H. Zhang, J. Zhao

State Key Laboratory of Nuclear Physics and Technology, Peking University, Beijing, China
A. Agapitos, Y. An, Y. Ban, C. Chen, A. Levin, Q. Li, X. Lyu, Y. Mao, S.J. Qian, D. Wang, J. Xiao

Sun Yat-Sen University, Guangzhou, China
M. Lu, Z. You

Institute of Modern Physics and Key Laboratory of Nuclear Physics and Ion-beam Application (MOE) - Fudan University, Shanghai, China
X. Gao[3], H. Okawa, Y. Zhang

Zhejiang University, Hangzhou, China, Zhejiang, China
Z. Lin, M. Xiao

Universidad de Los Andes, Bogota, Colombia
C. Avila, A. Cabrera, C. Florez, J. Fraga

Universidad de Antioquia, Medellin, Colombia
J. Mejia Guisao, F. Ramirez, J.D. Ruiz Alvarez, C.A. Salazar González

University of Split, Faculty of Electrical Engineering, Mechanical Engineering and Naval Architecture, Split, Croatia
D. Giljanovic, N. Godinovic, D. Lelas, I. Puljak

University of Split, Faculty of Science, Split, Croatia
Z. Antunovic, M. Kovac, T. Sculac

Institute Rudjer Boskovic, Zagreb, Croatia
V. Brigljevic, D. Ferencek, D. Majumder, M. Roguljic, A. Starodumov[12], T. Susa

University of Cyprus, Nicosia, Cyprus
A. Attikis, K. Christoforou, E. Erodotou, A. Ioannou, G. Kole, M. Kolosova, S. Konstantinou, J. Mousa, C. Nicolaou, F. Ptochos, P.A. Razis, H. Rykaczewski, H. Saka

Charles University, Prague, Czech Republic
M. Finger[13], M. Finger Jr.[13], A. Kveton

Escuela Politecnica Nacional, Quito, Ecuador
E. Ayala

Universidad San Francisco de Quito, Quito, Ecuador
E. Carrera Jarrin

Academy of Scientific Research and Technology of the Arab Republic of Egypt, Egyp-

tian Network of High Energy Physics, Cairo, Egypt
S. Elgammal[14], S. Khalil[15]

Center for High Energy Physics (CHEP-FU), Fayoum University, El-Fayoum, Egypt
M.A. Mahmoud, Y. Mohammed

National Institute of Chemical Physics and Biophysics, Tallinn, Estonia
S. Bhowmik, R.K. Dewanjee, K. Ehataht, M. Kadastik, S. Nandan, C. Nielsen, J. Pata, M. Raidal, L. Tani, C. Veelken

Department of Physics, University of Helsinki, Helsinki, Finland
P. Eerola, L. Forthomme, H. Kirschenmann, K. Osterberg, M. Voutilainen

Helsinki Institute of Physics, Helsinki, Finland
S. Bharthuar, E. Brücken, F. Garcia, J. Havukainen, M.S. Kim, R. Kinnunen, T. Lampén, K. Lassila-Perini, S. Lehti, T. Lindén, M. Lotti, L. Martikainen, M. Myllymäki, J. Ott, H. Siikonen, E. Tuominen, J. Tuominiemi

Lappeenranta University of Technology, Lappeenranta, Finland
P. Luukka, H. Petrow, T. Tuuva

IRFU, CEA, Université Paris-Saclay, Gif-sur-Yvette, France
C. Amendola, M. Besancon, F. Couderc, M. Dejardin, D. Denegri, J.L. Faure, F. Ferri, S. Ganjour, P. Gras, G. Hamel de Monchenault, P. Jarry, B. Lenzi, E. Locci, J. Malcles, J. Rander, A. Rosowsky, M.Ö. Sahin, A. Savoy-Navarro[16], M. Titov, G.B. Yu

Laboratoire Leprince-Ringuet, CNRS/IN2P3, Ecole Polytechnique, Institut Polytechnique de Paris, Palaiseau, France
S. Ahuja, F. Beaudette, M. Bonanomi, A. Buchot Perraguin, P. Busson, A. Cappati, C. Charlot, O. Davignon, B. Diab, G. Falmagne, S. Ghosh, R. Granier de Cassagnac, A. Hakimi, I. Kucher, J. Motta, M. Nguyen, C. Ochando, P. Paganini, J. Rembser, R. Salerno, U. Sarkar, J.B. Sauvan, Y. Sirois, A. Tarabini, A. Zabi, A. Zghiche

Université de Strasbourg, CNRS, IPHC UMR 7178, Strasbourg, France
J.-L. Agram[17], J. Andrea, D. Apparu, D. Bloch, G. Bourgatte, J.-M. Brom, E.C. Chabert, C. Collard, D. Darej, J.-C. Fontaine[17], U. Goerlach, C. Grimault, A.-C. Le Bihan, E. Nibigira, P. Van Hove

Institut de Physique des 2 Infinis de Lyon (IP2I), Villeurbanne, France
E. Asilar, S. Beauceron, C. Bernet, G. Boudoul, C. Camen, A. Carle, N. Chanon, D. Contardo, P. Depasse, H. El Mamouni, J. Fay, S. Gascon, M. Gouzevitch, B. Ille, I.B. Laktineh, H. Lattaud, A. Lesauvage, M. Lethuillier, L. Mirabito, S. Perries, K. Shchablo, V. Sordini, L. Torterotot, G. Touquet, M. Vander Donckt, S. Viret

Georgian Technical University, Tbilisi, Georgia
A. Khvedelidze[13], I. Lomidze, Z. Tsamalaidze[13]

RWTH Aachen University, I. Physikalisches Institut, Aachen, Germany
V. Botta, L. Feld, K. Klein, M. Lipinski, D. Meuser, A. Pauls, N. Röwert, J. Schulz, M. Teroerde

RWTH Aachen University, III. Physikalisches Institut A, Aachen, Germany
A. Dodonova, D. Eliseev, M. Erdmann, P. Fackeldey, B. Fischer, S. Ghosh, T. Hebbeker, K. Hoepfner, F. Ivone, L. Mastrolorenzo, M. Merschmeyer, A. Meyer, G. Mocellin, S. Mondal, S. Mukherjee, D. Noll, A. Novak, T. Pook, A. Pozdnyakov,

Y. Rath, H. Reithler, J. Roemer, A. Schmidt, S.C. Schuler, A. Sharma, L. Vigilante, S. Wiedenbeck, S. Zaleski

RWTH Aachen University, III. Physikalisches Institut B, Aachen, Germany
C. Dziwok, G. Flügge, W. Haj Ahmad[18], O. Hlushchenko, T. Kress, A. Nowack, C. Pistone, O. Pooth, D. Roy, A. Stahl[19], T. Ziemons, A. Zotz

Deutsches Elektronen-Synchrotron, Hamburg, Germany
H. Aarup Petersen, M. Aldaya Martin, P. Asmuss, S. Baxter, M. Bayatmakou, O. Behnke, A. Bermúdez Martínez, S. Bhattacharya, A.A. Bin Anuar, K. Borras[20], D. Brunner, A. Campbell, A. Cardini, C. Cheng, F. Colombina, S. Consuegra Rodríguez, G. Correia Silva, V. Danilov, M. De Silva, L. Didukh, G. Eckerlin, D. Eckstein, L.I. Estevez Banos, O. Filatov, E. Gallo[21], A. Geiser, A. Giraldi, A. Grohsjean, M. Guthoff, A. Jafari[22], N.Z. Jomhari, H. Jung, A. Kasem[20], M. Kasemann, H. Kaveh, C. Kleinwort, R. Kogler, D. Krücker, W. Lange, J. Lidrych, K. Lipka, W. Lohmann[23], R. Mankel, I.-A. Melzer-Pellmann, M. Mendizabal Morentin, J. Metwally, A.B. Meyer, M. Meyer, J. Mnich, A. Mussgiller, Y. Otarid, D. Pérez Adán, D. Pitzl, A. Raspereza, B. Ribeiro Lopes, J. Rübenach, A. Saggio, A. Saibel, M. Savitskyi, M. Scham[24], V. Scheurer, S. Schnake, P. Schütze, C. Schwanenberger[21], M. Shchedrolosiev, R.E. Sosa Ricardo, D. Stafford, N. Tonon, M. Van De Klundert, R. Walsh, D. Walter, Q. Wang, Y. Wen, K. Wichmann, L. Wiens, C. Wissing, S. Wuchterl

University of Hamburg, Hamburg, Germany
R. Aggleton, S. Albrecht, S. Bein, L. Benato, P. Connor, K. De Leo, M. Eich, F. Feindt, A. Fröhlich, C. Garbers, E. Garutti, P. Gunnellini, M. Hajheidari, J. Haller, A. Hinzmann, G. Kasieczka, R. Klanner, T. Kramer, V. Kutzner, J. Lange, T. Lange, A. Lobanov, A. Malara, A. Nigamova, K.J. Pena Rodriguez, M. Rieger, O. Rieger, P. Schleper, M. Schröder, J. Schwandt, J. Sonneveld, H. Stadie, G. Steinbrück, A. Tews, I. Zoi

Karlsruher Institut fuer Technologie, Karlsruhe, Germany
J. Bechtel, S. Brommer, M. Burkart, E. Butz, R. Caspart, T. Chwalek, W. De Boer[†], A. Dierlamm, A. Droll, K. El Morabit, N. Faltermann, M. Giffels, J.o. Gosewisch, A. Gottmann, F. Hartmann[19], C. Heidecker, U. Husemann, P. Keicher, R. Koppenhöfer, S. Maier, M. Metzler, S. Mitra, Th. Müller, M. Neukum, A. Nürnberg, G. Quast, K. Rabbertz, J. Rauser, D. Savoiu, M. Schnepf, D. Seith, I. Shvetsov, H.J. Simonis, R. Ulrich, J. Van Der Linden, R.F. Von Cube, M. Wassmer, M. Weber, S. Wieland, R. Wolf, S. Wozniewski, S. Wunsch

Institute of Nuclear and Particle Physics (INPP), NCSR Demokritos, Aghia Paraskevi, Greece
G. Anagnostou, G. Daskalakis, T. Geralis, A. Kyriakis, D. Loukas, A. Stakia

National and Kapodistrian University of Athens, Athens, Greece
M. Diamantopoulou, D. Karasavvas, G. Karathanasis, P. Kontaxakis, C.K. Koraka, A. Manousakis-Katsikakis, A. Panagiotou, I. Papavergou, N. Saoulidou, K. Theofilatos, E. Tziaferi, K. Vellidis, E. Vourliotis

National Technical University of Athens, Athens, Greece
G. Bakas, K. Kousouris, I. Papakrivopoulos, G. Tsipolitis, A. Zacharopoulou

University of Ioánnina, Ioánnina, Greece
K. Adamidis, I. Bestintzanos, I. Evangelou, C. Foudas, P. Gianneios, P. Katsoulis, P. Kokkas,

N. Manthos, I. Papadopoulos, J. Strologas

MTA-ELTE Lendület CMS Particle and Nuclear Physics Group, Eötvös Loránd University, Budapest, Hungary
M. Csanad, K. Farkas, M.M.A. Gadallah[25], S. Lökös[26], P. Major, K. Mandal, A. Mehta, G. Pasztor, A.J. Rádl, O. Surányi, G.I. Veres

Wigner Research Centre for Physics, Budapest, Hungary
M. Bartók[27], G. Bencze, C. Hajdu, D. Horvath[28], F. Sikler, V. Veszpremi

Institute of Nuclear Research ATOMKI, Debrecen, Hungary
S. Czellar, D. Fasanella, J. Karancsi[27], J. Molnar, Z. Szillasi, D. Teyssier

Institute of Physics, University of Debrecen, Debrecen, Hungary
P. Raics, Z.L. Trocsanyi[29], B. Ujvari

Karoly Robert Campus, MATE Institute of Technology, Gyongyos, Hungary
T. Csorgo[30], F. Nemes[30], T. Novak

Indian Institute of Science (IISc), Bangalore, India
S. Choudhury, J.R. Komaragiri, D. Kumar, L. Panwar, P.C. Tiwari

National Institute of Science Education and Research, HBNI, Bhubaneswar, India
S. Bahinipati[31], C. Kar, P. Mal, T. Mishra, V.K. Muraleedharan Nair Bindhu[32], A. Nayak[32], P. Saha, N. Sur, S.K. Swain, D. Vats[32]

Panjab University, Chandigarh, India
S. Bansal, S.B. Beri, V. Bhatnagar, G. Chaudhary, S. Chauhan, N. Dhingra[33], R. Gupta, A. Kaur, M. Kaur, S. Kaur, P. Kumari, M. Meena, K. Sandeep, J.B. Singh, A.K. Virdi

University of Delhi, Delhi, India
A. Ahmed, A. Bhardwaj, B.C. Choudhary, M. Gola, S. Keshri, A. Kumar, M. Naimuddin, P. Priyanka, K. Ranjan, A. Shah

Saha Institute of Nuclear Physics, HBNI, Kolkata, India
M. Bharti[34], R. Bhattacharya, S. Bhattacharya, D. Bhowmik, S. Dutta, S. Dutta, B. Gomber[35], M. Maity[36], P. Palit, P.K. Rout, G. Saha, B. Sahu, S. Sarkar, M. Sharan, B. Singh[34], S. Thakur[34]

Indian Institute of Technology Madras, Madras, India
P.K. Behera, S.C. Behera, P. Kalbhor, A. Muhammad, R. Pradhan, P.R. Pujahari, A. Sharma, A.K. Sikdar

Bhabha Atomic Research Centre, Mumbai, India
D. Dutta, V. Jha, V. Kumar, D.K. Mishra, K. Naskar[37], P.K. Netrakanti, L.M. Pant, P. Shukla

Tata Institute of Fundamental Research-A, Mumbai, India
T. Aziz, S. Dugad, M. Kumar, G.B. Mohanty

Tata Institute of Fundamental Research-B, Mumbai, India
S. Banerjee, R. Chudasama, M. Guchait, S. Karmakar, S. Kumar, G. Majumder, K. Mazumdar, S. Mukherjee

Indian Institute of Science Education and Research (IISER), Pune, India
K. Alpana, S. Dube, B. Kansal, A. Laha, S. Pandey, A. Rane, A. Rastogi, S. Sharma

Isfahan University of Technology, Isfahan, Iran
H. Bakhshiansohi[38], E. Khazaie, M. Zeinali[39]

Institute for Research in Fundamental Sciences (IPM), Tehran, Iran
S. Chenarani[40], S.M. Etesami, M. Khakzad, M. Mohammadi Najafabadi

University College Dublin, Dublin, Ireland
M. Grunewald

INFN Sezione di Bari [a], Bari, Italy, Università di Bari [b], Bari, Italy, Politecnico di Bari [c], Bari, Italy
M. Abbrescia[a,b], R. Aly[a,b,41], C. Aruta[a,b], A. Colaleo[a], D. Creanza[a,c], N. De Filippis[a,c], M. De Palma[a,b], A. Di Florio[a,b], A. Di Pilato[a,b], W. Elmetenawee[a,b], L. Fiore[a], A. Gelmi[a,b], M. Gul[a], G. Iaselli[a,c], M. Ince[a,b], S. Lezki[a,b], G. Maggi[a,c], M. Maggi[a], I. Margjeka[a,b], V. Mastrapasqua[a,b], S. My[a,b], S. Nuzzo[a,b], A. Pellecchia[a,b], A. Pompili[a,b], G. Pugliese[a,c], D. Ramos[a], A. Ranieri[a], G. Selvaggi[a,b], L. Silvestris[a], F.M. Simone[a,b], Ü. Sözbilir[a], R. Venditti[a], P. Verwilligen[a]

INFN Sezione di Bologna [a], Bologna, Italy, Università di Bologna [b], Bologna, Italy
G. Abbiendi[a], C. Battilana[a,b], D. Bonacorsi[a,b], L. Borgonovi[a], L. Brigliadori[a], R. Campanini[a,b], P. Capiluppi[a,b], A. Castro[a,b], F.R. Cavallo[a], M. Cuffiani[a,b], G.M. Dallavalle[a], T. Diotalevi[a,b], F. Fabbri[a], A. Fanfani[a,b], P. Giacomelli[a], L. Giommi[a,b], C. Grandi[a], L. Guiducci[a,b], S. Lo Meo[a,42], L. Lunerti[a,b], S. Marcellini[a], G. Masetti[a], F.L. Navarria[a,b], A. Perrotta[a], F. Primavera[a,b], A.M. Rossi[a,b], T. Rovelli[a,b], G.P. Siroli[a,b]

INFN Sezione di Catania [a], Catania, Italy, Università di Catania [b], Catania, Italy
S. Albergo[a,b,43], S. Costa[a,b,43], A. Di Mattia[a], R. Potenza[a,b], A. Tricomi[a,b,43], C. Tuve[a,b]

INFN Sezione di Firenze [a], Firenze, Italy, Università di Firenze [b], Firenze, Italy
G. Barbagli[a], A. Cassese[a], R. Ceccarelli[a,b], V. Ciulli[a,b], C. Civinini[a], R. D'Alessandro[a,b], E. Focardi[a,b], G. Latino[a,b], P. Lenzi[a,b], M. Lizzo[a,b], M. Meschini[a], S. Paoletti[a], R. Seidita[a,b], G. Sguazzoni[a], L. Viliani[a]

INFN Laboratori Nazionali di Frascati, Frascati, Italy
L. Benussi, S. Bianco, D. Piccolo

INFN Sezione di Genova [a], Genova, Italy, Università di Genova [b], Genova, Italy
M. Bozzo[a,b], F. Ferro[a], R. Mulargia[a,b], E. Robutti[a], S. Tosi[a,b]

INFN Sezione di Milano-Bicocca [a], Milano, Italy, Università di Milano-Bicocca [b], Milano, Italy
A. Benaglia[a], G. Boldrini, F. Brivio[a,b], F. Cetorelli[a,b], F. De Guio[a,b], M.E. Dinardo[a,b], P. Dini[a], S. Gennai[a], A. Ghezzi[a,b], P. Govoni[a,b], L. Guzzi[a,b], M.T. Lucchini[a,b], M. Malberti[a], S. Malvezzi[a], A. Massironi[a], D. Menasce[a], L. Moroni[a], M. Paganoni[a,b], D. Pedrini[a], B.S. Pinolini, S. Ragazzi[a,b], N. Redaelli[a], T. Tabarelli de Fatis[a,b], D. Valsecchi[a,b,19], D. Zuolo[a,b]

INFN Sezione di Napoli [a], Napoli, Italy, Università di Napoli 'Federico II' [b], Napoli, Italy, Università della Basilicata [c], Potenza, Italy, Università G. Marconi [d], Roma, Italy
S. Buontempo[a], F. Carnevali[a,b], N. Cavallo[a,c], A. De Iorio[a,b], F. Fabozzi[a,c], A.O.M. Iorio[a,b], L. Lista[a,b,44], S. Meola[a,d,19], P. Paolucci[a,19], B. Rossi[a], C. Sciacca[a,b]

INFN Sezione di Padova [a], Padova, Italy, Università di Padova [b], Padova, Italy, Università di Trento [c], Trento, Italy
P. Azzi[a], N. Bacchetta[a], D. Bisello[a,b], P. Bortignon[a], A. Bragagnolo[a,b], R. Carlin[a,b], P. Checchia[a], T. Dorigo[a], U. Dosselli[a], F. Gasparini[a,b], U. Gasparini[a,b], G. Grosso, S.Y. Hoh[a,b], L. Layer[a,45], E. Lusiani, M. Margoni[a,b], A.T. Meneguzzo[a,b], J. Pazzini[a,b], P. Ronchese[a,b], R. Rossin[a,b], F. Simonetto[a,b], G. Strong[a], M. Tosi[a,b], H. Yarar[a,b], M. Zanetti[a,b], P. Zotto[a,b], A. Zucchetta[a,b], G. Zumerle[a,b]

INFN Sezione di Pavia [a], Pavia, Italy, Università di Pavia [b], Pavia, Italy
C. Aime'[a,b], A. Braghieri[a], S. Calzaferri[a,b], D. Fiorina[a,b], P. Montagna[a,b], S.P. Ratti[a,b], V. Re[a], C. Riccardi[a,b], P. Salvini[a], I. Vai[a], P. Vitulo[a,b]

INFN Sezione di Perugia [a], Perugia, Italy, Università di Perugia [b], Perugia, Italy
P. Asenov[a,46], G.M. Bilei[a], D. Ciangottini[a,b], L. Fanò[a,b], M. Magherini[b], G. Mantovani[a,b], V. Mariani[a,b], M. Menichelli[a], F. Moscatelli[a,46], A. Piccinelli[a,b], M. Presilla[a,b], A. Rossi[a,b], A. Santocchia[a,b], D. Spiga[a], T. Tedeschi[a,b]

INFN Sezione di Pisa [a], Pisa, Italy, Università di Pisa [b], Pisa, Italy, Scuola Normale Superiore di Pisa [c], Pisa, Italy, Università di Siena [d], Siena, Italy
P. Azzurri[a], G. Bagliesi[a], V. Bertacchi[a,c], L. Bianchini[a], T. Boccali[a], E. Bossini[a,b], R. Castaldi[a], M.A. Ciocci[a,b], V. D'Amante[a,d], R. Dell'Orso[a], M.R. Di Domenico[a,d], S. Donato[a], A. Giassi[a], F. Ligabue[a,c], E. Manca[a,c], G. Mandorli[a,c], D. Matos Figueiredo, A. Messineo[a,b], F. Palla[a], S. Parolia[a,b], G. Ramirez-Sanchez[a,c], A. Rizzi[a,b], G. Rolandi[a,c], S. Roy Chowdhury[a,c], A. Scribano[a], N. Shafiei[a,b], P. Spagnolo[a], R. Tenchini[a], G. Tonelli[a,b], N. Turini[a,d], A. Venturi[a], P.G. Verdini[a]

INFN Sezione di Roma [a], Rome, Italy, Sapienza Università di Roma [b], Rome, Italy
P. Barria[a], M. Campana[a,b], F. Cavallari[a], D. Del Re[a,b], E. Di Marco[a], M. Diemoz[a], E. Longo[a,b], P. Meridiani[a], G. Organtini[a,b], F. Pandolfi[a], R. Paramatti[a,b], C. Quaranta[a,b], S. Rahatlou[a,b], C. Rovelli[a], F. Santanastasio[a,b], L. Soffi[a], R. Tramontano[a,b]

INFN Sezione di Torino [a], Torino, Italy, Università di Torino [b], Torino, Italy, Università del Piemonte Orientale [c], Novara, Italy
N. Amapane[a,b], R. Arcidiacono[a,c], S. Argiro[a,b], M. Arneodo[a,c], N. Bartosik[a], R. Bellan[a,b], A. Bellora[a,b], J. Berenguer Antequera[a,b], C. Biino[a], N. Cartiglia[a], S. Cometti[a], M. Costa[a,b], R. Covarelli[a,b], N. Demaria[a], B. Kiani[a,b], F. Legger[a], C. Mariotti[a], S. Maselli[a], E. Migliore[a,b], E. Monteil[a,b], M. Monteno[a], M.M. Obertino[a,b], G. Ortona[a], L. Pacher[a,b], N. Pastrone[a], M. Pelliccioni[a], G.L. Pinna Angioni[a,b], M. Ruspa[a,c], K. Shchelina[a], F. Siviero[a,b], V. Sola[a], A. Solano[a,b], D. Soldi[a,b], A. Staiano[a], M. Tornago[a,b], D. Trocino[a], A. Vagnerini[a,b]

INFN Sezione di Trieste [a], Trieste, Italy, Università di Trieste [b], Trieste, Italy
S. Belforte[a], V. Candelise[a,b], M. Casarsa[a], F. Cossutti[a], A. Da Rold[a,b], G. Della Ricca[a,b], G. Sorrentino[a,b], F. Vazzoler[a,b]

Kyungpook National University, Daegu, Korea
S. Dogra, C. Huh, B. Kim, D.H. Kim, G.N. Kim, J. Kim, J. Lee, S.W. Lee, C.S. Moon, Y.D. Oh, S.I. Pak, B.C. Radburn-Smith, S. Sekmen, Y.C. Yang

Chonnam National University, Institute for Universe and Elementary Particles, Kwangju, Korea

H. Kim, D.H. Moon

Hanyang University, Seoul, Korea
B. Francois, T.J. Kim, J. Park

Korea University, Seoul, Korea
S. Cho, S. Choi, Y. Go, B. Hong, K. Lee, K.S. Lee, J. Lim, J. Park, S.K. Park, J. Yoo

Kyung Hee University, Department of Physics, Seoul, Republic of Korea, Seoul, Korea
J. Goh, A. Gurtu

Sejong University, Seoul, Korea
H.S. Kim, Y. Kim

Seoul National University, Seoul, Korea
J. Almond, J.H. Bhyun, J. Choi, S. Jeon, J. Kim, J.S. Kim, S. Ko, H. Kwon, H. Lee, S. Lee, B.H. Oh, M. Oh, S.B. Oh, H. Seo, U.K. Yang, I. Yoon

University of Seoul, Seoul, Korea
W. Jang, D.Y. Kang, Y. Kang, S. Kim, B. Ko, J.S.H. Lee, Y. Lee, J.A. Merlin, I.C. Park, Y. Roh, M.S. Ryu, D. Song, I.J. Watson, S. Yang

Yonsei University, Department of Physics, Seoul, Korea
S. Ha, H.D. Yoo

Sungkyunkwan University, Suwon, Korea
M. Choi, H. Lee, Y. Lee, I. Yu

College of Engineering and Technology, American University of the Middle East (AUM), Egaila, Kuwait, Dasman, Kuwait
T. Beyrouthy, Y. Maghrbi

Riga Technical University, Riga, Latvia
K. Dreimanis, V. Veckalns[47]

Vilnius University, Vilnius, Lithuania
M. Ambrozas, A. Carvalho Antunes De Oliveira, A. Juodagalvis, A. Rinkevicius, G. Tamulaitis

National Centre for Particle Physics, Universiti Malaya, Kuala Lumpur, Malaysia
N. Bin Norjoharuddeen, W.A.T. Wan Abdullah, M.N. Yusli, Z. Zolkapli

Universidad de Sonora (UNISON), Hermosillo, Mexico
J.F. Benitez, A. Castaneda Hernandez, M. León Coello, J.A. Murillo Quijada, A. Sehrawat, L. Valencia Palomo

Centro de Investigacion y de Estudios Avanzados del IPN, Mexico City, Mexico
G. Ayala, H. Castilla-Valdez, E. De La Cruz-Burelo, I. Heredia-De La Cruz[48], R. Lopez-Fernandez, C.A. Mondragon Herrera, D.A. Perez Navarro, A. Sánchez Hernández

Universidad Iberoamericana, Mexico City, Mexico
S. Carrillo Moreno, C. Oropeza Barrera, F. Vazquez Valencia

Benemerita Universidad Autonoma de Puebla, Puebla, Mexico
I. Pedraza, H.A. Salazar Ibarguen, C. Uribe Estrada

University of Montenegro, Podgorica, Montenegro
J. Mijuskovic[49], N. Raicevic

University of Auckland, Auckland, New Zealand
D. Krofcheck

University of Canterbury, Christchurch, New Zealand
P.H. Butler

National Centre for Physics, Quaid-I-Azam University, Islamabad, Pakistan
A. Ahmad, M.I. Asghar, A. Awais, M.I.M. Awan, H.R. Hoorani, W.A. Khan, M.A. Shah, M. Shoaib, M. Waqas

AGH University of Science and Technology Faculty of Computer Science, Electronics and Telecommunications, Krakow, Poland
V. Avati, L. Grzanka, M. Malawski

National Centre for Nuclear Research, Swierk, Poland
H. Bialkowska, M. Bluj, B. Boimska, M. Górski, M. Kazana, M. Szleper, P. Zalewski

Institute of Experimental Physics, Faculty of Physics, University of Warsaw, Warsaw, Poland
K. Bunkowski, K. Doroba, A. Kalinowski, M. Konecki, J. Krolikowski

Laboratório de Instrumentação e Física Experimental de Partículas, Lisboa, Portugal
M. Araujo, P. Bargassa, D. Bastos, A. Boletti, P. Faccioli, M. Gallinaro, J. Hollar, N. Leonardo, T. Niknejad, M. Pisano, J. Seixas, O. Toldaiev, J. Varela

Joint Institute for Nuclear Research, Dubna, Russia
S. Afanasiev, D. Budkouski, I. Golutvin, I. Gorbunov, V. Karjavine, V. Korenkov, A. Lanev, A. Malakhov, V. Matveev[50,51], V. Palichik, V. Perelygin, M. Savina, D. Seitova, V. Shalaev, S. Shmatov, S. Shulha, V. Smirnov, O. Teryaev, N. Voytishin, B.S. Yuldashev[52], A. Zarubin, I. Zhizhin

Petersburg Nuclear Physics Institute, Gatchina (St. Petersburg), Russia
G. Gavrilov, V. Golovtcov, Y. Ivanov, V. Kim[53], E. Kuznetsova[54], V. Murzin, V. Oreshkin, I. Smirnov, D. Sosnov, V. Sulimov, L. Uvarov, S. Volkov, A. Vorobyev

Institute for Nuclear Research, Moscow, Russia
Yu. Andreev, A. Dermenev, S. Gninenko, N. Golubev, A. Karneyeu, D. Kirpichnikov, M. Kirsanov, N. Krasnikov, A. Pashenkov, G. Pivovarov, A. Toropin

Moscow Institute of Physics and Technology, Moscow, Russia
T. Aushev

National Research Center 'Kurchatov Institute', Moscow, Russia
V. Epshteyn, V. Gavrilov, N. Lychkovskaya, A. Nikitenko[55], V. Popov, A. Stepennov, M. Toms, E. Vlasov, A. Zhokin

National Research Nuclear University 'Moscow Engineering Physics Institute' (MEPhI), Moscow, Russia
O. Bychkova, R. Chistov[56], M. Danilov[57], A. Oskin, P. Parygin, S. Polikarpov[57]

P.N. Lebedev Physical Institute, Moscow, Russia
V. Andreev, M. Azarkin, I. Dremin, M. Kirakosyan, A. Terkulov

Skobeltsyn Institute of Nuclear Physics, Lomonosov Moscow State University, Moscow, Russia
A. Belyaev, E. Boos, V. Bunichev, M. Dubinin[58], L. Dudko, A. Ershov, A. Gribushin, V. Klyukhin, O. Kodolova, I. Lokhtin, S. Obraztsov, S. Petrushanko, V. Savrin

Novosibirsk State University (NSU), Novosibirsk, Russia
V. Blinov[59], T. Dimova[59], L. Kardapoltsev[59], A. Kozyrev[59], I. Ovtin[59], O. Radchenko[59], Y. Skovpen[59]

Institute for High Energy Physics of National Research Centre 'Kurchatov Institute', Protvino, Russia
I. Azhgirey, I. Bayshev, D. Elumakhov, V. Kachanov, D. Konstantinov, P. Mandrik, V. Petrov, R. Ryutin, S. Slabospitskii, A. Sobol, S. Troshin, N. Tyurin, A. Uzunian, A. Volkov

National Research Tomsk Polytechnic University, Tomsk, Russia
A. Babaev, V. Okhotnikov

Tomsk State University, Tomsk, Russia
V. Borshch, V. Ivanchenko, E. Tcherniaev

University of Belgrade: Faculty of Physics and VINCA Institute of Nuclear Sciences, Belgrade, Serbia
P. Adzic[60], M. Dordevic, P. Milenovic, J. Milosevic

Centro de Investigaciones Energéticas Medioambientales y Tecnológicas (CIEMAT), Madrid, Spain
M. Aguilar-Benitez, J. Alcaraz Maestre, A. Álvarez Fernández, I. Bachiller, M. Barrio Luna, Cristina F. Bedoya, C.A. Carrillo Montoya, M. Cepeda, M. Cerrada, N. Colino, B. De La Cruz, A. Delgado Peris, J.P. Fernández Ramos, J. Flix, M.C. Fouz, O. Gonzalez Lopez, S. Goy Lopez, J.M. Hernandez, M.I. Josa, J. León Holgado, D. Moran, Á. Navarro Tobar, C. Perez Dengra, A. Pérez-Calero Yzquierdo, J. Puerta Pelayo, I. Redondo, L. Romero, S. Sánchez Navas, L. Urda Gómez, C. Willmott

Universidad Autónoma de Madrid, Madrid, Spain
J.F. de Trocóniz, R. Reyes-Almanza

Universidad de Oviedo, Instituto Universitario de Ciencias y Tecnologías Espaciales de Asturias (ICTEA), Oviedo, Spain
B. Alvarez Gonzalez, J. Cuevas, C. Erice, J. Fernandez Menendez, S. Folgueras, I. Gonzalez Caballero, J.R. González Fernández, E. Palencia Cortezon, C. Ramón Álvarez, V. Rodríguez Bouza, A. Soto Rodríguez, A. Trapote, N. Trevisani, C. Vico Villalba

Instituto de Física de Cantabria (IFCA), CSIC-Universidad de Cantabria, Santander, Spain
J.A. Brochero Cifuentes, I.J. Cabrillo, A. Calderon, J. Duarte Campderros, M. Fernandez, C. Fernandez Madrazo, P.J. Fernández Manteca, A. García Alonso, G. Gomez, C. Martinez Rivero, P. Martinez Ruiz del Arbol, F. Matorras, P. Matorras Cuevas, J. Piedra Gomez, C. Prieels, T. Rodrigo, A. Ruiz-Jimeno, L. Scodellaro, I. Vila, J.M. Vizan Garcia

University of Colombo, Colombo, Sri Lanka
M.K. Jayananda, B. Kailasapathy[61], D.U.J. Sonnadara, D.D.C. Wickramarathna

University of Ruhuna, Department of Physics, Matara, Sri Lanka
W.G.D. Dharmaratna, K. Liyanage, N. Perera, N. Wickramage

CERN, European Organization for Nuclear Research, Geneva, Switzerland
T.K. Aarrestad, D. Abbaneo, J. Alimena, E. Auffray, G. Auzinger, J. Baechler, P. Baillon[†], D. Barney, J. Bendavid, M. Bianco, A. Bocci, T. Camporesi, M. Capeans Garrido, G. Cerminara, N. Chernyavskaya, S.S. Chhibra, M. Cipriani, L. Cristella, D. d'Enterria, A. Dabrowski, A. David, A. De Roeck, M.M. Defranchis, M. Deile,

M. Dobson, M. Dünser, N. Dupont, A. Elliott-Peisert, N. Emriskova, F. Fallavollita[62], A. Florent, G. Franzoni, W. Funk, S. Giani, D. Gigi, K. Gill, F. Glege, L. Gouskos, M. Haranko, J. Hegeman, V. Innocente, T. James, P. Janot, J. Kaspar, J. Kieseler, M. Komm, N. Kratochwil, C. Lange, S. Laurila, P. Lecoq, A. Lintuluoto, K. Long, C. Lourenço, B. Maier, L. Malgeri, S. Mallios, M. Mannelli, A.C. Marini, F. Meijers, S. Mersi, E. Meschi, F. Moortgat, M. Mulders, S. Orfanelli, L. Orsini, F. Pantaleo, E. Perez, M. Peruzzi, A. Petrilli, G. Petrucciani, A. Pfeiffer, M. Pierini, D. Piparo, M. Pitt, H. Qu, T. Quast, D. Rabady, A. Racz, G. Reales Gutiérrez, M. Rovere, H. Sakulin, J. Salfeld-Nebgen, S. Scarfi, C. Schäfer, C. Schwick, M. Selvaggi, A. Sharma, P. Silva, W. Snoeys, P. Sphicas[63], S. Summers, K. Tatar, V.R. Tavolaro, D. Treille, P. Tropea, A. Tsirou, G.P. Van Onsem, J. Wanczyk[64], K.A. Wozniak, W.D. Zeuner

Paul Scherrer Institut, Villigen, Switzerland
L. Caminada[65], A. Ebrahimi, W. Erdmann, R. Horisberger, Q. Ingram, H.C. Kaestli, D. Kotlinski, U. Langenegger, M. Missiroli[65], L. Noehte[65], T. Rohe

ETH Zurich - Institute for Particle Physics and Astrophysics (IPA), Zurich, Switzerland
K. Androsov[64], M. Backhaus, P. Berger, A. Calandri, A. De Cosa, G. Dissertori, M. Dittmar, M. Donegà, C. Dorfer, F. Eble, K. Gedia, F. Glessgen, T.A. Gómez Espinosa, C. Grab, D. Hits, W. Lustermann, A.-M. Lyon, R.A. Manzoni, L. Marchese, C. Martin Perez, M.T. Meinhard, F. Nessi-Tedaldi, J. Niedziela, F. Pauss, V. Perovic, S. Pigazzini, M.G. Ratti, M. Reichmann, C. Reissel, T. Reitenspiess, B. Ristic, D. Ruini, D.A. Sanz Becerra, V. Stampf, J. Steggemann[64], R. Wallny, D.H. Zhu

Universität Zürich, Zurich, Switzerland
C. Amsler[66], P. Bärtschi, C. Botta, D. Brzhechko, M.F. Canelli, K. Cormier, A. De Wit, R. Del Burgo, J.K. Heikkilä, M. Huwiler, W. Jin, A. Jofrehei, B. Kilminster, S. Leontsinis, S.P. Liechti, A. Macchiolo, P. Meiring, V.M. Mikuni, U. Molinatti, I. Neutelings, A. Reimers, P. Robmann, S. Sanchez Cruz, K. Schweiger, M. Senger, Y. Takahashi

National Central University, Chung-Li, Taiwan
C. Adloff[67], C.M. Kuo, W. Lin, A. Roy, T. Sarkar[36], S.S. Yu

National Taiwan University (NTU), Taipei, Taiwan
L. Ceard, Y. Chao, K.F. Chen, P.H. Chen, W.-S. Hou, Y.y. Li, R.-S. Lu, E. Paganis, A. Psallidas, A. Steen, H.y. Wu, E. Yazgan, P.r. Yu

Chulalongkorn University, Faculty of Science, Department of Physics, Bangkok, Thailand
B. Asavapibhop, C. Asawatangtrakuldee, N. Srimanobhas

Çukurova University, Physics Department, Science and Art Faculty, Adana, Turkey
F. Boran, S. Damarseckin[68], Z.S. Demiroglu, F. Dolek, I. Dumanoglu[69], E. Eskut, Y. Guler[70], E. Gurpinar Guler[70], C. Isik, O. Kara, A. Kayis Topaksu, U. Kiminsu, G. Onengut, K. Ozdemir[71], A. Polatoz, A.E. Simsek, B. Tali[72], U.G. Tok, S. Turkcapar, I.S. Zorbakir

Middle East Technical University, Physics Department, Ankara, Turkey
B. Isildak[73], G. Karapinar, K. Ocalan[74], M. Yalvac[75]

Bogazici University, Istanbul, Turkey
B. Akgun, I.O. Atakisi, E. Gülmez, M. Kaya[76], O. Kaya[77], Ö. Özçelik, S. Tekten[78], E.A. Yetkin[79]

Istanbul Technical University, Istanbul, Turkey
A. Cakir, K. Cankocak[69], Y. Komurcu, S. Sen[80]

Istanbul University, Istanbul, Turkey
S. Cerci[72], I. Hos[81], B. Kaynak, S. Ozkorucuklu, H. Sert, D. Sunar Cerci[72], C. Zorbilmez

Institute for Scintillation Materials of National Academy of Science of Ukraine, Kharkov, Ukraine
B. Grynyov

National Scientific Center, Kharkov Institute of Physics and Technology, Kharkov, Ukraine
L. Levchuk

University of Bristol, Bristol, United Kingdom
D. Anthony, E. Bhal, S. Bologna, J.J. Brooke, A. Bundock, E. Clement, D. Cussans, H. Flacher, J. Goldstein, G.P. Heath, H.F. Heath, L. Kreczko, B. Krikler, S. Paramesvaran, S. Seif El Nasr-Storey, V.J. Smith, N. Stylianou[82], K. Walkingshaw Pass, R. White

Rutherford Appleton Laboratory, Didcot, United Kingdom
K.W. Bell, A. Belyaev[83], C. Brew, R.M. Brown, D.J.A. Cockerill, C. Cooke, K.V. Ellis, K. Harder, S. Harper, M.-L. Holmberg[84], J. Linacre, K. Manolopoulos, D.M. Newbold, E. Olaiya, D. Petyt, T. Reis, T. Schuh, C.H. Shepherd-Themistocleous, I.R. Tomalin, T. Williams

Imperial College, London, United Kingdom
R. Bainbridge, P. Bloch, S. Bonomally, J. Borg, S. Breeze, O. Buchmuller, V. Cepaitis, G.S. Chahal[85], D. Colling, P. Dauncey, G. Davies, M. Della Negra, S. Fayer, G. Fedi, G. Hall, M.H. Hassanshahi, G. Iles, J. Langford, L. Lyons, A.-M. Magnan, S. Malik, A. Martelli, D.G. Monk, J. Nash[86], M. Pesaresi, D.M. Raymond, A. Richards, A. Rose, E. Scott, C. Seez, A. Shtipliyski, A. Tapper, K. Uchida, T. Virdee[19], M. Vojinovic, N. Wardle, S.N. Webb, D. Winterbottom

Brunel University, Uxbridge, United Kingdom
K. Coldham, J.E. Cole, A. Khan, P. Kyberd, I.D. Reid, L. Teodorescu, S. Zahid

Baylor University, Waco, Texas, USA
S. Abdullin, A. Brinkerhoff, B. Caraway, J. Dittmann, K. Hatakeyama, A.R. Kanuganti, B. McMaster, N. Pastika, M. Saunders, S. Sawant, C. Sutantawibul, J. Wilson

Catholic University of America, Washington, DC, USA
R. Bartek, A. Dominguez, R. Uniyal, A.M. Vargas Hernandez

The University of Alabama, Tuscaloosa, Alabama, USA
A. Buccilli, S.I. Cooper, D. Di Croce, S.V. Gleyzer, C. Henderson, C.U. Perez, P. Rumerio[87], C. West

Boston University, Boston, Massachusetts, USA
A. Akpinar, A. Albert, D. Arcaro, C. Cosby, Z. Demiragli, E. Fontanesi, D. Gastler, S. May, J. Rohlf, K. Salyer, D. Sperka, D. Spitzbart, I. Suarez, A. Tsatsos, S. Yuan, D. Zou

Brown University, Providence, Rhode Island, USA
G. Benelli, B. Burkle, X. Coubez[20], D. Cutts, M. Hadley, U. Heintz, J.M. Hogan[88],

T. KWON, G. Landsberg, K.T. Lau, D. Li, M. Lukasik, J. Luo, M. Narain, N. Pervan, S. Sagir[89], F. Simpson, E. Usai, W.Y. Wong, X. Yan, D. Yu, W. Zhang

University of California, Davis, Davis, California, USA
J. Bonilla, C. Brainerd, R. Breedon, M. Calderon De La Barca Sanchez, M. Chertok, J. Conway, P.T. Cox, R. Erbacher, G. Haza, F. Jensen, O. Kukral, R. Lander, M. Mulhearn, D. Pellett, B. Regnery, D. Taylor, Y. Yao, F. Zhang

University of California, Los Angeles, California, USA
M. Bachtis, R. Cousins, A. Datta, D. Hamilton, J. Hauser, M. Ignatenko, M.A. Iqbal, T. Lam, W.A. Nash, S. Regnard, D. Saltzberg, B. Stone, V. Valuev

University of California, Riverside, Riverside, California, USA
K. Burt, Y. Chen, R. Clare, J.W. Gary, M. Gordon, G. Hanson, G. Karapostoli, O.R. Long, N. Manganelli, M. Olmedo Negrete, W. Si, S. Wimpenny, Y. Zhang

University of California, San Diego, La Jolla, California, USA
J.G. Branson, P. Chang, S. Cittolin, S. Cooperstein, N. Deelen, D. Diaz, J. Duarte, R. Gerosa, L. Giannini, J. Guiang, R. Kansal, V. Krutelyov, R. Lee, J. Letts, M. Masciovecchio, F. Mokhtar, M. Pieri, B.V. Sathia Narayanan, V. Sharma, M. Tadel, A. Vartak, F. Würthwein, Y. Xiang, A. Yagil

University of California, Santa Barbara - Department of Physics, Santa Barbara, California, USA
N. Amin, C. Campagnari, M. Citron, A. Dorsett, V. Dutta, J. Incandela, M. Kilpatrick, J. Kim, B. Marsh, H. Mei, M. Oshiro, M. Quinnan, J. Richman, U. Sarica, F. Setti, J. Sheplock, P. Siddireddy, D. Stuart, S. Wang

California Institute of Technology, Pasadena, California, USA
A. Bornheim, O. Cerri, I. Dutta, J.M. Lawhorn, N. Lu, J. Mao, H.B. Newman, T.Q. Nguyen, M. Spiropulu, J.R. Vlimant, C. Wang, S. Xie, Z. Zhang, R.Y. Zhu

Carnegie Mellon University, Pittsburgh, Pennsylvania, USA
J. Alison, S. An, M.B. Andrews, P. Bryant, T. Ferguson, A. Harilal, C. Liu, T. Mudholkar, M. Paulini, A. Sanchez, W. Terrill

University of Colorado Boulder, Boulder, Colorado, USA
J.P. Cumalat, W.T. Ford, A. Hassani, E. MacDonald, R. Patel, A. Perloff, C. Savard, K. Stenson, K.A. Ulmer, S.R. Wagner

Cornell University, Ithaca, New York, USA
J. Alexander, S. Bright-Thonney, X. Chen, Y. Cheng, D.J. Cranshaw, S. Hogan, J. Monroy, J.R. Patterson, D. Quach, J. Reichert, M. Reid, A. Ryd, W. Sun, J. Thom, P. Wittich, R. Zou

Fermi National Accelerator Laboratory, Batavia, Illinois, USA
M. Albrow, M. Alyari, G. Apollinari, A. Apresyan, A. Apyan, S. Banerjee, L.A.T. Bauerdick, D. Berry, J. Berryhill, P.C. Bhat, K. Burkett, J.N. Butler, A. Canepa, G.B. Cerati, H.W.K. Cheung, F. Chlebana, K.F. Di Petrillo, V.D. Elvira, Y. Feng, J. Freeman, Z. Gecse, L. Gray, D. Green, S. Grünendahl, O. Gutsche, R.M. Harris, R. Heller, T.C. Herwig, J. Hirschauer, B. Jayatilaka, S. Jindariani, M. Johnson, U. Joshi, T. Klijnsma, B. Klima, K.H.M. Kwok, S. Lammel, D. Lincoln, R. Lipton, T. Liu, C. Madrid, K. Maeshima, C. Mantilla, D. Mason, P. McBride, P. Merkel, S. Mrenna, S. Nahn, J. Ngadiuba, V. O'Dell, V. Papadimitriou, K. Pedro, C. Pena[58], O. Prokofyev,

F. Ravera, A. Reinsvold Hall, L. Ristori, E. Sexton-Kennedy, N. Smith, A. Soha, W.J. Spalding, L. Spiegel, S. Stoynev, J. Strait, L. Taylor, S. Tkaczyk, N.V. Tran, L. Uplegger, E.W. Vaandering, H.A. Weber

University of Florida, Gainesville, Florida, USA
D. Acosta, P. Avery, D. Bourilkov, L. Cadamuro, V. Cherepanov, F. Errico, R.D. Field, D. Guerrero, B.M. Joshi, M. Kim, E. Koenig, J. Konigsberg, A. Korytov, K.H. Lo, K. Matchev, N. Menendez, G. Mitselmakher, A. Muthirakalayil Madhu, N. Rawal, D. Rosenzweig, S. Rosenzweig, J. Rotter, K. Shi, J. Sturdy, J. Wang, E. Yigitbasi, X. Zuo

Florida State University, Tallahassee, Florida, USA
T. Adams, A. Askew, R. Habibullah, V. Hagopian, K.F. Johnson, R. Khurana, T. Kolberg, G. Martinez, H. Prosper, C. Schiber, O. Viazlo, R. Yohay, J. Zhang

Florida Institute of Technology, Melbourne, Florida, USA
M.M. Baarmand, S. Butalla, T. Elkafrawy[90], M. Hohlmann, R. Kumar Verma, D. Noonan, M. Rahmani, F. Yumiceva

University of Illinois at Chicago (UIC), Chicago, Illinois, USA
M.R. Adams, H. Becerril Gonzalez, R. Cavanaugh, S. Dittmer, O. Evdokimov, C.E. Gerber, D.A. Hangal, D.J. Hofman, A.H. Merrit, C. Mills, G. Oh, T. Roy, S. Rudrabhatla, M.B. Tonjes, N. Varelas, J. Viinikainen, X. Wang, Z. Wu, Z. Ye

The University of Iowa, Iowa City, Iowa, USA
M. Alhusseini, K. Dilsiz[91], L. Emediato, R.P. Gandrajula, O.K. Köseyan, J.-P. Merlo, A. Mestvirishvili[92], J. Nachtman, H. Ogul[93], Y. Onel, A. Penzo, C. Snyder, E. Tiras[94]

Johns Hopkins University, Baltimore, Maryland, USA
O. Amram, B. Blumenfeld, L. Corcodilos, J. Davis, M. Eminizer, A.V. Gritsan, S. Kyriacou, P. Maksimovic, J. Roskes, M. Swartz, T.Á. Vámi

The University of Kansas, Lawrence, Kansas, USA
A. Abreu, J. Anguiano, C. Baldenegro Barrera, P. Baringer, A. Bean, A. Bylinkin, Z. Flowers, T. Isidori, S. Khalil, J. King, G. Krintiras, A. Kropivnitskaya, M. Lazarovits, C. Le Mahieu, C. Lindsey, J. Marquez, N. Minafra, M. Murray, M. Nickel, C. Rogan, C. Royon, R. Salvatico, S. Sanders, E. Schmitz, C. Smith, J.D. Tapia Takaki, Q. Wang, Z. Warner, J. Williams, G. Wilson

Kansas State University, Manhattan, Kansas, USA
S. Duric, A. Ivanov, K. Kaadze, D. Kim, Y. Maravin, T. Mitchell, A. Modak, K. Nam

Lawrence Livermore National Laboratory, Livermore, California, USA
F. Rebassoo, D. Wright

University of Maryland, College Park, Maryland, USA
E. Adams, A. Baden, O. Baron, A. Belloni, S.C. Eno, N.J. Hadley, S. Jabeen, R.G. Kellogg, T. Koeth, S. Lascio, A.C. Mignerey, S. Nabili, C. Palmer, M. Seidel, A. Skuja, L. Wang, K. Wong

Massachusetts Institute of Technology, Cambridge, Massachusetts, USA
D. Abercrombie, G. Andreassi, R. Bi, W. Busza, I.A. Cali, Y. Chen, M. D'Alfonso, J. Eysermans, C. Freer, G. Gomez Ceballos, M. Goncharov, P. Harris, M. Hu, M. Klute, D. Kovalskyi, J. Krupa, Y.-J. Lee, C. Mironov, C. Paus, D. Rankin, C. Roland, G. Roland, Z. Shi, G.S.F. Stephans, J. Wang, Z. Wang, B. Wyslouch

University of Minnesota, Minneapolis, Minnesota, USA
R.M. Chatterjee, A. Evans, J. Hiltbrand, Sh. Jain, M. Krohn, Y. Kubota, J. Mans, M. Revering, R. Rusack, R. Saradhy, N. Schroeder, N. Strobbe, M.A. Wadud

University of Nebraska-Lincoln, Lincoln, Nebraska, USA
K. Bloom, M. Bryson, S. Chauhan, D.R. Claes, C. Fangmeier, L. Finco, F. Golf, C. Joo, I. Kravchenko, M. Musich, I. Reed, J.E. Siado, G.R. Snow†, W. Tabb, F. Yan, A.G. Zecchinelli

State University of New York at Buffalo, Buffalo, New York, USA
G. Agarwal, H. Bandyopadhyay, L. Hay, I. Iashvili, A. Kharchilava, C. McLean, D. Nguyen, J. Pekkanen, S. Rappoccio, A. Williams

Northeastern University, Boston, Massachusetts, USA
G. Alverson, E. Barberis, Y. Haddad, A. Hortiangtham, J. Li, G. Madigan, B. Marzocchi, D.M. Morse, V. Nguyen, T. Orimoto, A. Parker, L. Skinnari, A. Tishelman-Charny, T. Wamorkar, B. Wang, A. Wisecarver, D. Wood

Northwestern University, Evanston, Illinois, USA
S. Bhattacharya, J. Bueghly, Z. Chen, A. Gilbert, T. Gunter, K.A. Hahn, Y. Liu, N. Odell, M.H. Schmitt, M. Velasco

University of Notre Dame, Notre Dame, Indiana, USA
R. Band, R. Bucci, M. Cremonesi, A. Das, N. Dev, R. Goldouzian, M. Hildreth, K. Hurtado Anampa, C. Jessop, K. Lannon, J. Lawrence, N. Loukas, D. Lutton, J. Mariano, N. Marinelli, I. Mcalister, T. McCauley, C. Mcgrady, K. Mohrman, C. Moore, Y. Musienko[50], R. Ruchti, A. Townsend, M. Wayne, A. Wightman, M. Zarucki, L. Zygala

The Ohio State University, Columbus, Ohio, USA
B. Bylsma, B. Cardwell, L.S. Durkin, B. Francis, C. Hill, M. Nunez Ornelas, K. Wei, B.L. Winer, B.R. Yates

Princeton University, Princeton, New Jersey, USA
F.M. Addesa, B. Bonham, P. Das, G. Dezoort, P. Elmer, A. Frankenthal, B. Greenberg, N. Haubrich, S. Higginbotham, A. Kalogeropoulos, G. Kopp, S. Kwan, D. Lange, D. Marlow, K. Mei, I. Ojalvo, J. Olsen, D. Stickland, C. Tully

University of Puerto Rico, Mayaguez, Puerto Rico, USA
S. Malik, S. Norberg

Purdue University, West Lafayette, Indiana, USA
A.S. Bakshi, V.E. Barnes, R. Chawla, S. Das, L. Gutay, M. Jones, A.W. Jung, S. Karmarkar, D. Kondratyev, M. Liu, G. Negro, N. Neumeister, G. Paspalaki, S. Piperov, A. Purohit, J.F. Schulte, M. Stojanovic[16], J. Thieman, F. Wang, R. Xiao, W. Xie

Purdue University Northwest, Hammond, Indiana, USA
J. Dolen, N. Parashar

Rice University, Houston, Texas, USA
A. Baty, T. Carnahan, M. Decaro, S. Dildick, K.M. Ecklund, S. Freed, P. Gardner, F.J.M. Geurts, A. Kumar, W. Li, B.P. Padley, R. Redjimi, W. Shi, A.G. Stahl Leiton, S. Yang, L. Zhang[95], Y. Zhang

University of Rochester, Rochester, New York, USA
A. Bodek, P. de Barbaro, R. Demina, J.L. Dulemba, C. Fallon, T. Ferbel, M. Galanti,

A. Garcia-Bellido, O. Hindrichs, A. Khukhunaishvili, E. Ranken, R. Taus

Rutgers, The State University of New Jersey, Piscataway, New Jersey, USA
B. Chiarito, J.P. Chou, A. Gandrakota, Y. Gershtein, E. Halkiadakis, A. Hart, M. Heindl, O. Karacheban[23], I. Laflotte, A. Lath, R. Montalvo, K. Nash, M. Osherson, S. Salur, S. Schnetzer, S. Somalwar, R. Stone, S.A. Thayil, S. Thomas, H. Wang

University of Tennessee, Knoxville, Tennessee, USA
H. Acharya, A.G. Delannoy, S. Fiorendi, S. Spanier

Texas A&M University, College Station, Texas, USA
O. Bouhali[96], M. Dalchenko, A. Delgado, R. Eusebi, J. Gilmore, T. Huang, T. Kamon[97], H. Kim, S. Luo, S. Malhotra, R. Mueller, D. Overton, D. Rathjens, A. Safonov

Texas Tech University, Lubbock, Texas, USA
N. Akchurin, J. Damgov, V. Hegde, S. Kunori, K. Lamichhane, S.W. Lee, T. Mengke, S. Muthumuni, T. Peltola, I. Volobouev, Z. Wang, A. Whitbeck

Vanderbilt University, Nashville, Tennessee, USA
E. Appelt, S. Greene, A. Gurrola, W. Johns, A. Melo, H. Ni, K. Padeken, F. Romeo, P. Sheldon, S. Tuo, J. Velkovska

University of Virginia, Charlottesville, Virginia, USA
M.W. Arenton, B. Cox, G. Cummings, J. Hakala, R. Hirosky, M. Joyce, A. Ledovskoy, A. Li, C. Neu, C.E. Perez Lara, B. Tannenwald, S. White, E. Wolfe

Wayne State University, Detroit, Michigan, USA
N. Poudyal

University of Wisconsin - Madison, Madison, WI, Wisconsin, USA
K. Black, T. Bose, C. Caillol, S. Dasu, I. De Bruyn, P. Everaerts, F. Fienga, C. Galloni, H. He, M. Herndon, A. Hervé, U. Hussain, A. Lanaro, A. Loeliger, R. Loveless, J. Madhusudanan Sreekala, A. Mallampalli, A. Mohammadi, D. Pinna, A. Savin, V. Shang, V. Sharma, W.H. Smith, D. Teague, S. Trembath-Reichert, W. Vetens

†: Deceased
1: Also at TU Wien, Wien, Austria
2: Also at Institute of Basic and Applied Sciences, Faculty of Engineering, Arab Academy for Science, Technology and Maritime Transport, Alexandria, Egypt
3: Also at Université Libre de Bruxelles, Bruxelles, Belgium
4: Also at Universidade Estadual de Campinas, Campinas, Brazil
5: Also at Federal University of Rio Grande do Sul, Porto Alegre, Brazil
6: Also at The University of the State of Amazonas, Manaus, Brazil
7: Also at University of Chinese Academy of Sciences, Beijing, China
8: Also at Department of Physics, Tsinghua University, Beijing, China
9: Also at UFMS, Nova Andradina, Brazil
10: Also at Nanjing Normal University Department of Physics, Nanjing, China
11: Now at The University of Iowa, Iowa City, Iowa, USA
12: Also at National Research Center 'Kurchatov Institute', Moscow, Russia
13: Also at Joint Institute for Nuclear Research, Dubna, Russia
14: Now at British University in Egypt, Cairo, Egypt
15: Also at Zewail City of Science and Technology, Zewail, Egypt
16: Also at Purdue University, West Lafayette, Indiana, USA
17: Also at Université de Haute Alsace, Mulhouse, France

18: Also at Erzincan Binali Yildirim University, Erzincan, Turkey
19: Also at CERN, European Organization for Nuclear Research, Geneva, Switzerland
20: Also at RWTH Aachen University, III. Physikalisches Institut A, Aachen, Germany
21: Also at University of Hamburg, Hamburg, Germany
22: Also at Isfahan University of Technology, Isfahan, Iran
23: Also at Brandenburg University of Technology, Cottbus, Germany
24: Also at Forschungszentrum Jülich, Juelich, Germany
25: Also at Physics Department, Faculty of Science, Assiut University, Assiut, Egypt
26: Also at Karoly Robert Campus, MATE Institute of Technology, Gyongyos, Hungary
27: Also at Institute of Physics, University of Debrecen, Debrecen, Hungary
28: Also at Institute of Nuclear Research ATOMKI, Debrecen, Hungary
29: Also at MTA-ELTE Lendület CMS Particle and Nuclear Physics Group, Eötvös Loránd University, Budapest, Hungary
30: Also at Wigner Research Centre for Physics, Budapest, Hungary
31: Also at IIT Bhubaneswar, Bhubaneswar, India
32: Also at Institute of Physics, Bhubaneswar, India
33: Also at Punjab Agricultural University, Ludhiana, India
34: Also at Shoolini University, Solan, India
35: Also at University of Hyderabad, Hyderabad, India
36: Also at University of Visva-Bharati, Santiniketan, India
37: Also at Indian Institute of Technology (IIT), Mumbai, India
38: Also at Deutsches Elektronen-Synchrotron, Hamburg, Germany
39: Also at Sharif University of Technology, Tehran, Iran
40: Also at Department of Physics, University of Science and Technology of Mazandaran, Behshahr, Iran
41: Now at INFN Sezione di Bari, Università di Bari, Politecnico di Bari, Bari, Italy
42: Also at Italian National Agency for New Technologies, Energy and Sustainable Economic Development, Bologna, Italy
43: Also at Centro Siciliano di Fisica Nucleare e di Struttura Della Materia, Catania, Italy
44: Also at Scuola Superiore Meridionale, Università di Napoli Federico II, Napoli, Italy
45: Also at Università di Napoli 'Federico II', Napoli, Italy
46: Also at Consiglio Nazionale delle Ricerche - Istituto Officina dei Materiali, Perugia, Italy
47: Also at Riga Technical University, Riga, Latvia
48: Also at Consejo Nacional de Ciencia y Tecnología, Mexico City, Mexico
49: Also at IRFU, CEA, Université Paris-Saclay, Gif-sur-Yvette, France
50: Also at Institute for Nuclear Research, Moscow, Russia
51: Now at National Research Nuclear University 'Moscow Engineering Physics Institute' (MEPhI), Moscow, Russia
52: Also at Institute of Nuclear Physics of the Uzbekistan Academy of Sciences, Tashkent, Uzbekistan
53: Also at St. Petersburg Polytechnic University, St. Petersburg, Russia
54: Also at University of Florida, Gainesville, Florida, USA
55: Also at Imperial College, London, United Kingdom
56: Also at Moscow Institute of Physics and Technology, Moscow, Russia
57: Also at P.N. Lebedev Physical Institute, Moscow, Russia
58: Also at California Institute of Technology, Pasadena, California, USA
59: Also at Budker Institute of Nuclear Physics, Novosibirsk, Russia
60: Also at Faculty of Physics, University of Belgrade, Belgrade, Serbia
61: Also at Trincomalee Campus, Eastern University, Sri Lanka, Nilaveli, Sri Lanka

62: Also at INFN Sezione di Pavia, Università di Pavia, Pavia, Italy
63: Also at National and Kapodistrian University of Athens, Athens, Greece
64: Also at Ecole Polytechnique Fédérale Lausanne, Lausanne, Switzerland
65: Also at Universität Zürich, Zurich, Switzerland
66: Also at Stefan Meyer Institute for Subatomic Physics, Vienna, Austria
67: Also at Laboratoire d'Annecy-le-Vieux de Physique des Particules, IN2P3-CNRS, Annecy-le-Vieux, France
68: Also at Şırnak University, Sirnak, Turkey
69: Also at Near East University, Research Center of Experimental Health Science, Nicosia, Turkey
70: Also at Konya Technical University, Konya, Turkey
71: Also at Piri Reis University, Istanbul, Turkey
72: Also at Adiyaman University, Adiyaman, Turkey
73: Also at Ozyegin University, Istanbul, Turkey
74: Also at Necmettin Erbakan University, Konya, Turkey
75: Also at Bozok Universitetesi Rektörlügü, Yozgat, Turkey
76: Also at Marmara University, Istanbul, Turkey
77: Also at Milli Savunma University, Istanbul, Turkey
78: Also at Kafkas University, Kars, Turkey
79: Also at Istanbul Bilgi University, Istanbul, Turkey
80: Also at Hacettepe University, Ankara, Turkey
81: Also at Istanbul University - Cerrahpasa, Faculty of Engineering, Istanbul, Turkey
82: Also at Vrije Universiteit Brussel, Brussel, Belgium
83: Also at School of Physics and Astronomy, University of Southampton, Southampton, United Kingdom
84: Also at Rutherford Appleton Laboratory, Didcot, United Kingdom
85: Also at IPPP Durham University, Durham, United Kingdom
86: Also at Monash University, Faculty of Science, Clayton, Australia
87: Also at Università di Torino, Torino, Italy
88: Also at Bethel University, St. Paul, Minneapolis, USA
89: Also at Karamanoğlu Mehmetbey University, Karaman, Turkey
90: Also at Ain Shams University, Cairo, Egypt
91: Also at Bingol University, Bingol, Turkey
92: Also at Georgian Technical University, Tbilisi, Georgia
93: Also at Sinop University, Sinop, Turkey
94: Also at Erciyes University, Kayseri, Turkey
95: Also at Institute of Modern Physics and Key Laboratory of Nuclear Physics and Ion-beam Application (MOE) - Fudan University, Shanghai, China
96: Also at Texas A&M University at Qatar, Doha, Qatar
97: Also at Kyungpook National University, Daegu, Korea